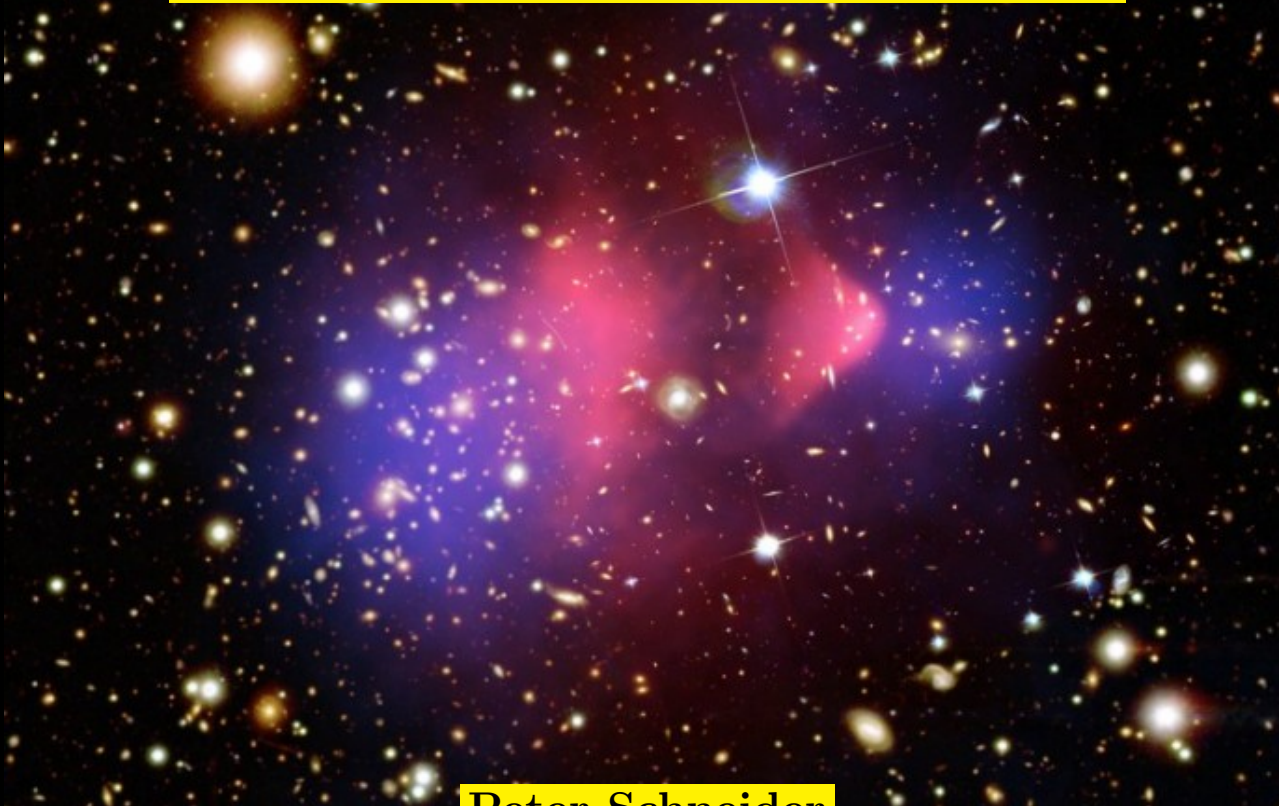


# Gravitational lensing: A powerful cosmological tool

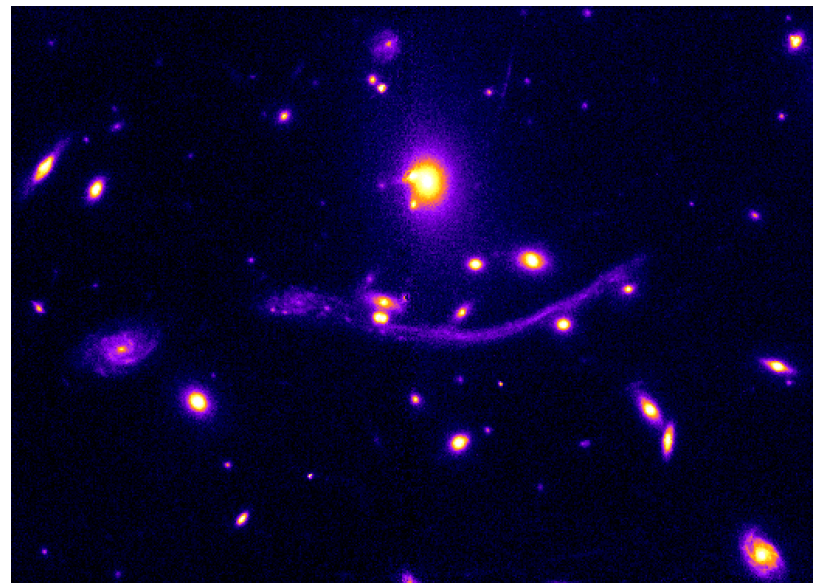
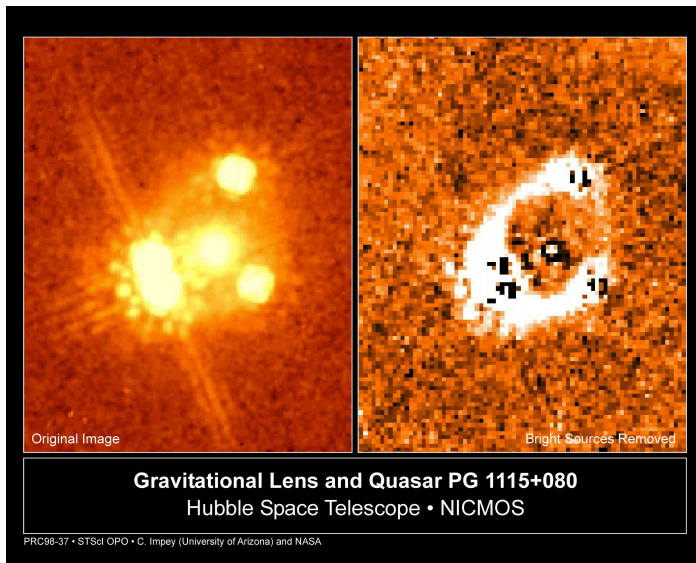


Peter Schneider

Argelander-Institut für Astronomie, Universität Bonn

# Gravitational light deflection ...

- ... independent of nature and state of deflecting matter
- ... causes changes of apparent position; multiple imaging
- ... differential light deflection causes magnification and shape distortion



The gravitational lens effect can be used to learn something

- about the lens
  - e.g., mass distribution
- about the source
  - e.g., brightness distribution
- about the geometry of space between source, lens, and observer
  - e.g., the geometry of the Universe and its expansion history.

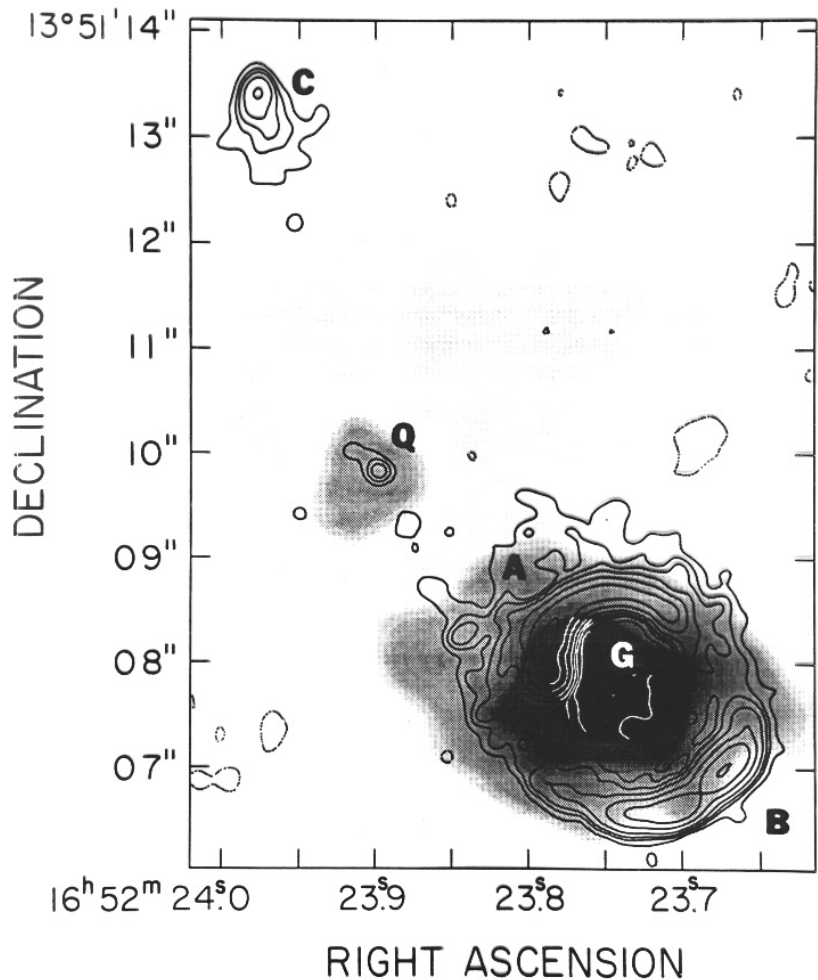
## Einstein rings

If

- the mass distribution is approximately spherically symmetric,
- sufficiently well concentrated, and
- the source is located directly behind lens,

then a ring-shaped image of the lens is formed: **Einstein rings**.

Langston et al. (1988)



## Two slides of Basics

Mass inside the Einstein ring ( $\theta_E$ ) follows from  $\alpha(\xi) = \frac{4GM(<\xi)}{c^2\xi}$ :

$$M(< D_d\theta_E) = \frac{c^2 D_s}{4\pi G D_d D_{ds}} (D_d\theta_E)^2 \pi =: \Sigma_{cr} (D_d\theta_E)^2 \pi$$

By far the most accurate mass determination in extragalactic astronomy!

$D$ 's: (angular-diameter) distances between observer, deflector and source;

$\Sigma_{cr}$ : **critical surface mass density**, depends on lens and source redshift;  
used to scale surface mass densities,

$$\kappa(\boldsymbol{\theta}) = \frac{\Sigma(D_d\boldsymbol{\theta})}{\Sigma_{cr}} : \text{ dimensionless surface mass density, or } \text{convergence};$$

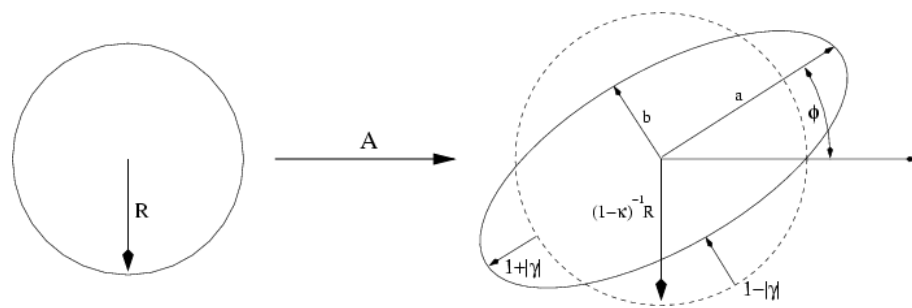
$|\kappa| \ll 1$  corresponds to **weak lensing** (image distortions, small magnifications),  
 $\kappa \gtrsim 1$  to **strong lensing** (multiple images, giant arcs, large magnifications).

**Tidal effects** of light deflection described by **shear**  $\gamma$ ;

Shear linearly related to convergence  $\kappa$ , most easily written in Fourier space,

$$\hat{\gamma}(\ell) = \hat{\kappa}(\ell) \exp(2i \text{ phase of } \ell)$$

Small circular source of radius  $\theta$  (to first order) mapped into ellipse, with semi-axis  $\theta/(1 - \kappa \pm |\gamma|)$ ; orientation given by phase of  $\gamma$



**Magnification** of images of *small sources* is  $\mu = \frac{1}{(1 - \kappa)^2 - |\gamma|^2}$  ;

for extended sources, magnification depends on source size and light profile.  
Magnification renders images larger and brighter (at conserved surface brightness)

# This talk: Selection of recent results

- Mass distribution in galaxies
- Properties of cluster mass distributions
- Natural telescopes
- Lensing by the LSS
- Biasing of galaxies

# Strong lensing by galaxies

## Selection of candidate lens systems mainly by:

- Image configuration (multiple images, arcs, rings), in optical or radio surveys
- Spectroscopy: Two redshifts in a single spectrum (e.g., SLACS)
- Extreme apparent luminosity

## Selected applications and results:

- Slope of the mass profile;  
contribution of DM to the mass inside  $\theta_E$
- $M/L$  for the stellar components – clues to IMF
- Ellipticity of the mass distribution – follows light?
- Independent determination of  $H_0$ , from time delays in multiple image systems

# The unfortunate mass-sheet degeneracy

For a given source and lens redshift:

The mass distributions  $\kappa(\boldsymbol{\theta})$  and, for all  $\lambda$ ,

$$\kappa_\lambda(\boldsymbol{\theta}) := \lambda\kappa(\boldsymbol{\theta}) + (1 - \lambda)$$

yield **the same** image configurations, magnification ratios, image shapes!

Magnification depends on  $\lambda$ ,  $\mu_\lambda = \mu/\lambda^2$  – but unmeasurable without information about the source (or source population)

Time-delay affected,  $(H_0 \Delta t)_\lambda = \lambda(H_0 \Delta t)$

Radial slope of density profile affected

Invariant: (Mass inside) Einstein radius, angular structure (e.g., ellipticity)

**Thus:**

**To determine slope of mass profile, absolute masses (away from the Einstein radius), Hubble constant, mass-sheet degeneracy must first be broken!!**

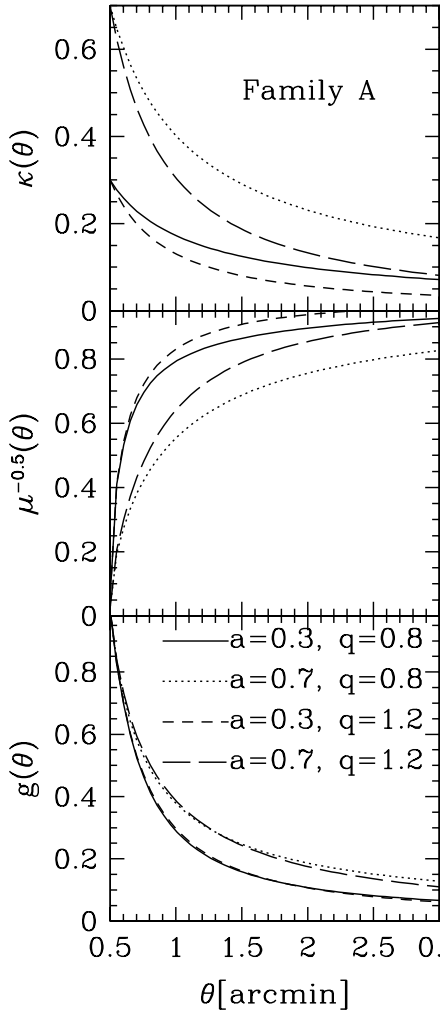


## Illustration of mass-sheet degeneracy:

Four different mass distributions (top – all local power laws) lead to pairwise almost degenerate weak lensing observable  $g$  (bottom).

Magnification information can break this degeneracy, but requires very accurate external calibration.

Schneider et al. (2000)

# How to break the mass-sheet degeneracy

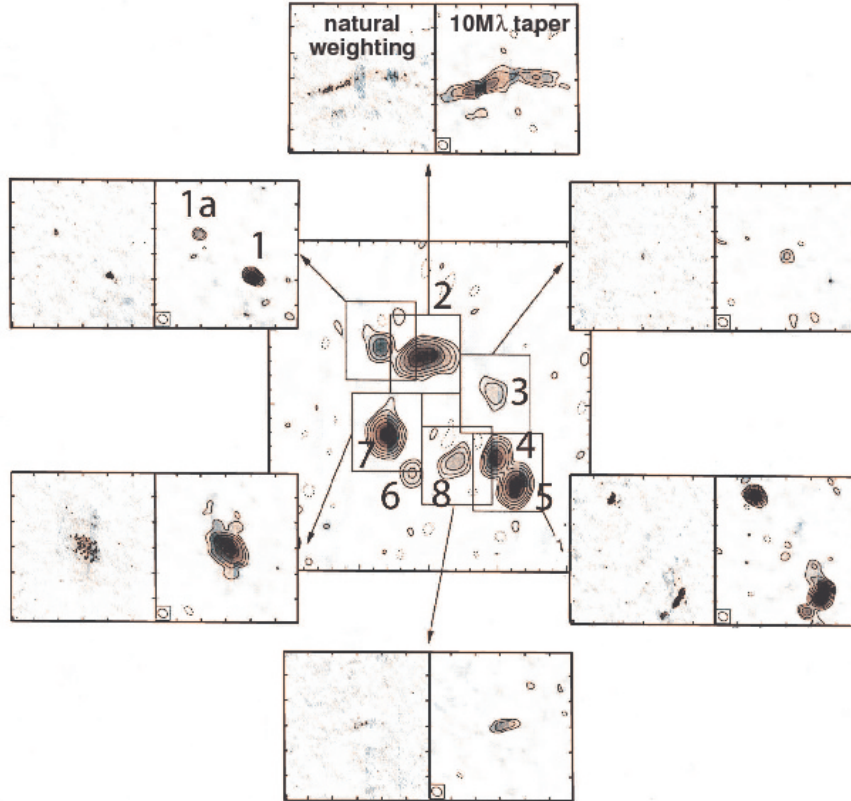
- Assume a parametrized mass model (e.g., power law, or NFW, for  $\kappa$ )
- Assume  $\kappa \rightarrow 0$  (or  $\kappa \rightarrow \kappa_{\text{NFW}}$ ) for large separation from lens center
- Use independent mass probes – e.g., stellar dynamics in galaxies
- Assume ‘mass follows light’ on average, for clusters
- Have independent information about source size or luminosity (e.g., fundamental plane)
- Employ statistical distribution of source properties (e.g., number counts for large-scale cluster lensing)
- MSD partly broken if sources at vastly different (and known) redshifts are lensed by the same mass concentration (e.g., multiple arc systems in clusters)

These methods are ‘more or less’ successful ...

MSD remains the **largest obstacle** for model-independent accurate results.

For galaxy lenses, stellar dynamical techniques have been most successful.

# Case study: B1933+503



A ten ( $= 4 + 4 + 2$ ) image lens system in the radio

MERLIN (center) and global VLBI image at 18 cm

Suyu et al. (2012)



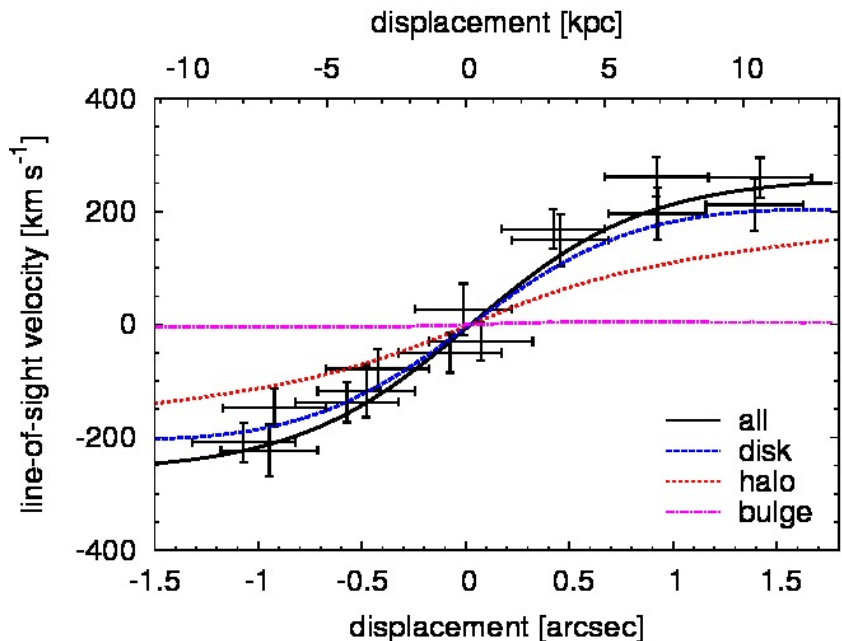
B1933 in HST optical + ground-based K-band composite

component 6 is reddened by dust absorption

Suyu et al. (2012)

Lens model = disk + triaxial NFW halo + bulge

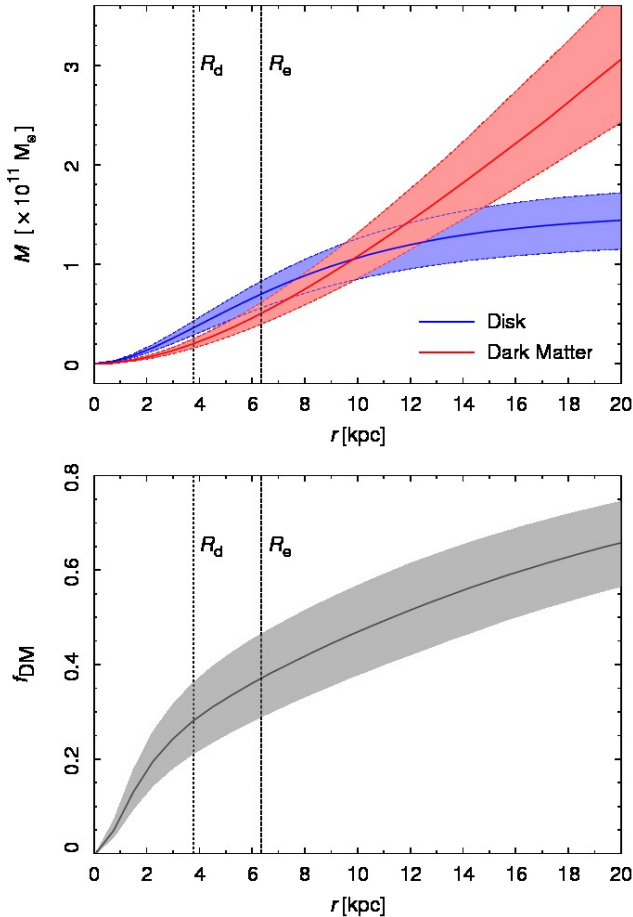
Constraints: image position and rotation curve (breaks MSD!)



Resulting model fits rotation curve well

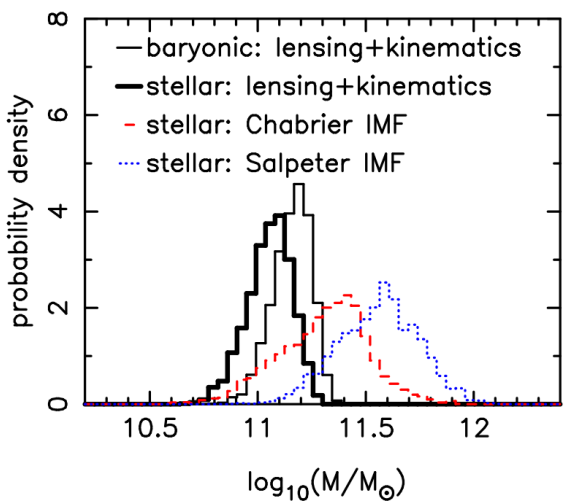
also reproduces the image positions

Suyu et al. (2012)



## Results:

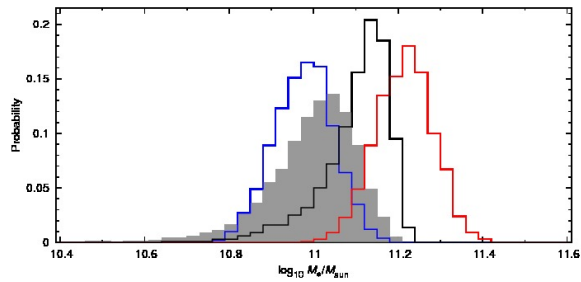
- Projected mass distribution of halo has axis ratio  $0.67 \pm 0.04$
- If axisymmetric, DM halo oblate with  $a/c = 0.33 \pm 0.06$ : presence of disk leads to inner halo flattening
- DM mass fraction inside effective radius:  $f_{\text{DM},e} = 0.37 \pm 0.08$
- disk contributes  $\sim (75 \pm 5)\%$  to rotation velocity at  $2.2R_d$ : disk not maximal
- $\log(M_*/M_\odot) = 11.06 \pm 0.10$  (if 20% gas is assumed)



Comparison of stellar mass obtained from lensing + kinematics with stellar mass obtained from population synthesis yields:

A bottom-heavy IMF is strongly disfavoured in this system;

Suyu et al. (2012)



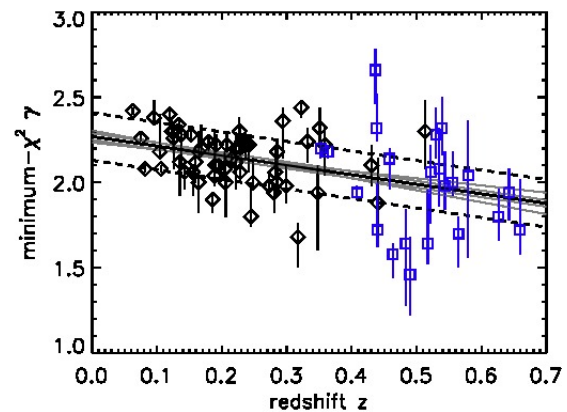
Similar result also found in other spiral lenses;  
a Salpeter IMF strongly disfavoured (SWELLS survey)

Barnabè et al. (2012)

# Recent results

- Determination of Hubble constant,  $H_0 = (71 \pm 3)$  km/s/Mpc (Suyu et al. 2010)  
**Note:** Independent  $H_0$ -determinations are most valuable to break cosmological parameter degeneracies from CMB anisotropies.
- Slope of the mass profile close to isothermal,  $\rho(r) \propto r^{-\gamma}$ , with  $\gamma \sim 2$
- Indications for slope getting steeper at higher redshift

Bolton et al. (2012); SLACS & BELLS samples,  
also seen in SL2S sample



- Dark matter fraction within effective radius:  
 $\sim 30\%$  for Salpeter IMF,  $\sim 60\%$  for Chabrier IMF;  
DM fraction increases with increasing total mass (Barnabè et al. 2011)

# Weak lensing

**Shear** (tidal component of the deflection) causes distortion of images;  
in terms of ellipticity,

$$\epsilon \approx \epsilon^s + \gamma ;$$

orientation of sources is random,  $\langle \epsilon^s \rangle = 0 \Rightarrow \langle \epsilon \rangle = \gamma / (1 - \kappa)$ :

The image of every galaxy provides an unbiased (but noisy!) estimate of the reduced shear  $g = \gamma / (1 - \kappa)$ .

Necessarily a statistical approach:  $\sigma(\epsilon^s) \gg$  typical shears

Main problem: how to measure  $\epsilon$  of faint galaxy images and correct for PSF and pixelization effect?

**Major progress** achieved in recent years (e.g., GREAT10, Kitching et al. 2012)

Recall:  $\kappa$  and  $\gamma$  are linearly related

$\Rightarrow$  a measured shear field can be transformed into a  $\kappa$  map.

**Magnification** changes the local source counts:

If a source population has counts  $n_0(> S)$ , then a magnification  $\mu$  yields

$$n(> S) = \frac{1}{\mu} n_0 \left( > \frac{S}{\mu} \right)$$

e.g., for power law  $n_0(> S) \propto S^{-\beta} \Rightarrow n(> S) = \mu^{(\beta-1)} n_0(> S)$ :

Enhancement or decrease of source density, depending on slope  $\beta$ .

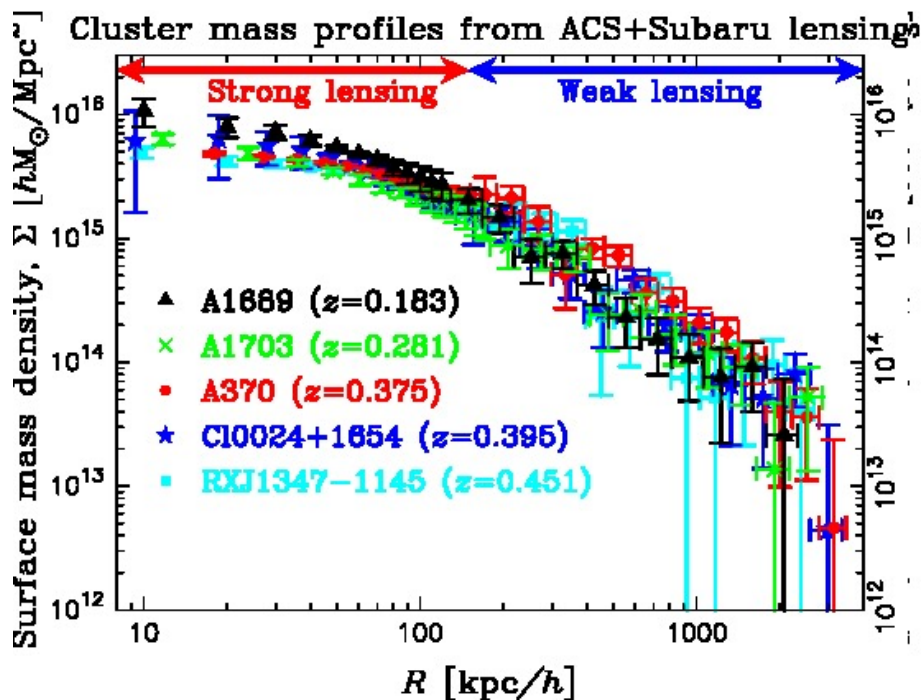
Advantage: breaks mass-sheet degeneracy, but only if  $n_0(> S)$  is well known.

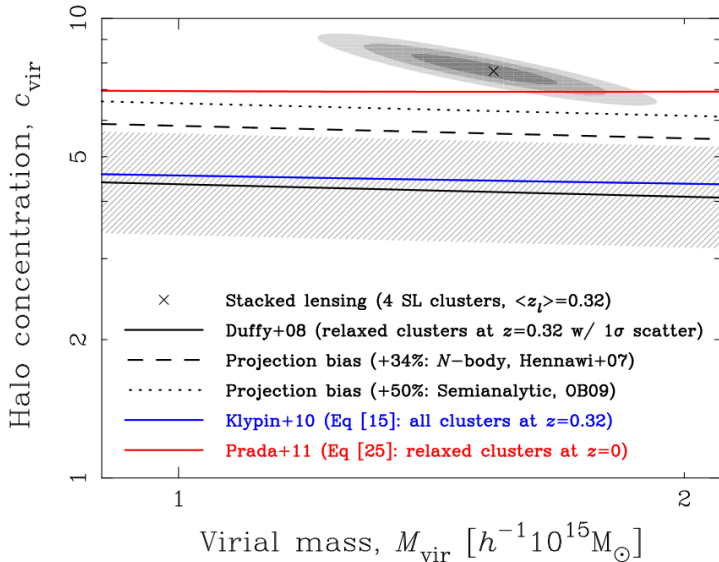
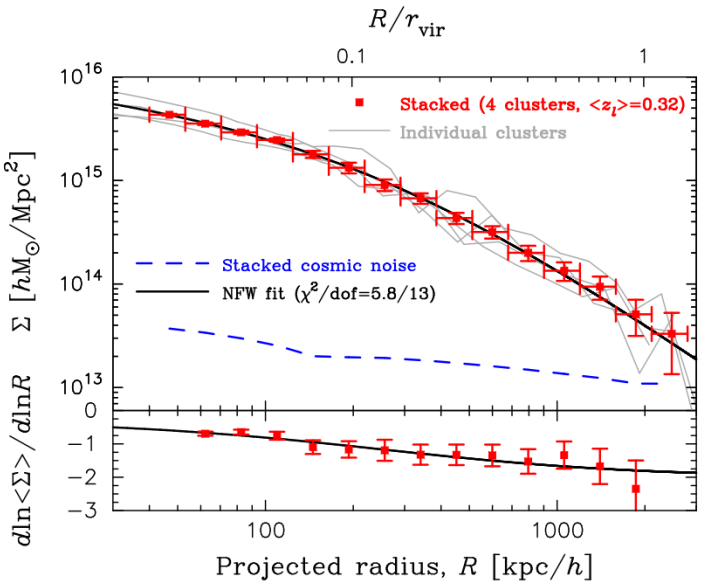
Difficulties: Calibration issues, source clustering, contamination (e.g., by cluster galaxies)

# The mean density profile of clusters

Umetsu et al. (2011a, b) studied 5 (4) strong lensing clusters using shear + magnification bias (number counts) + strong lensing:

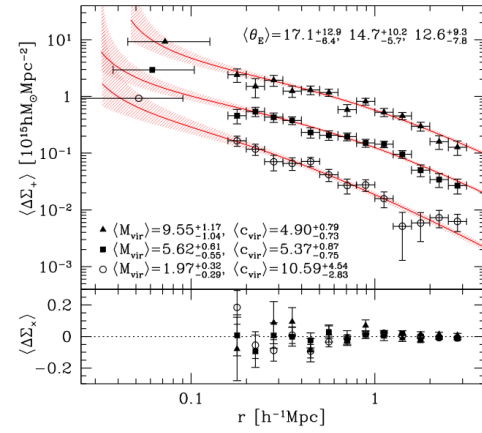
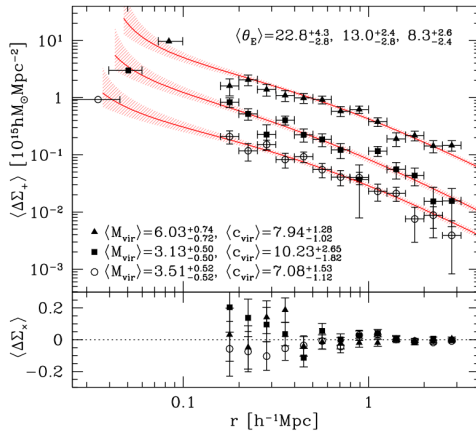
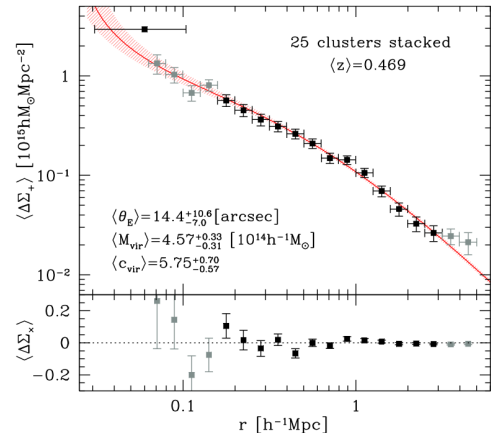
Mass profiles of these 5 clusters:





- NFW-profile fits remarkably well! Too well?
- Mean concentration parameter is  $c \approx 7.7$ , slightly higher than expected in 3-D, from DM-only simulations
- $c$  biased high due to strong lensing selection

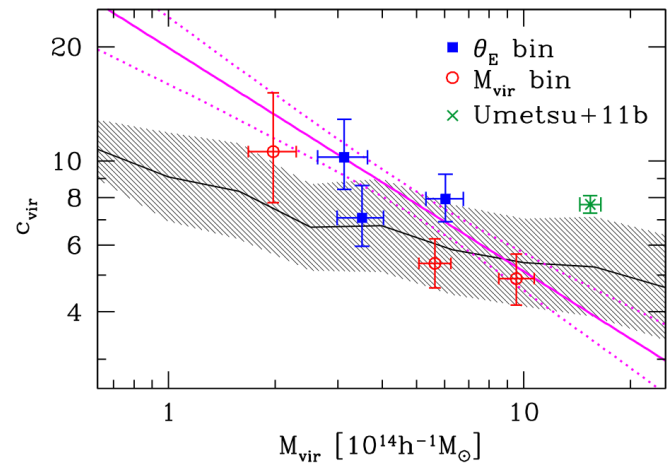
Oguri (2011) used 28 clusters from Sloan Giant Arcs Survey; shear only



all clusters

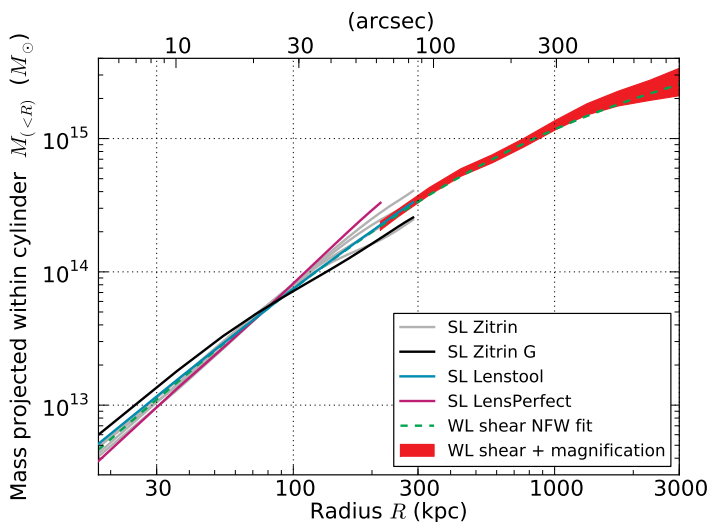
$\theta_E$  bins

$M_{\text{vir}}$  bins



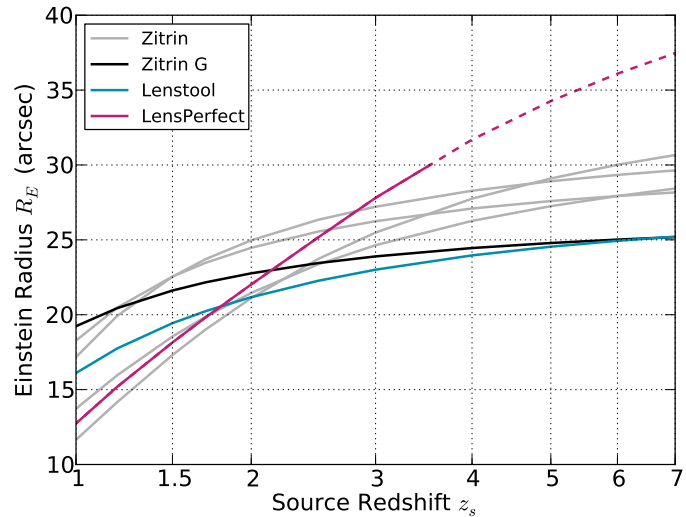
NFW-concentration,  
compared to expectations including selection  
bias

## How unique are these mass profiles?



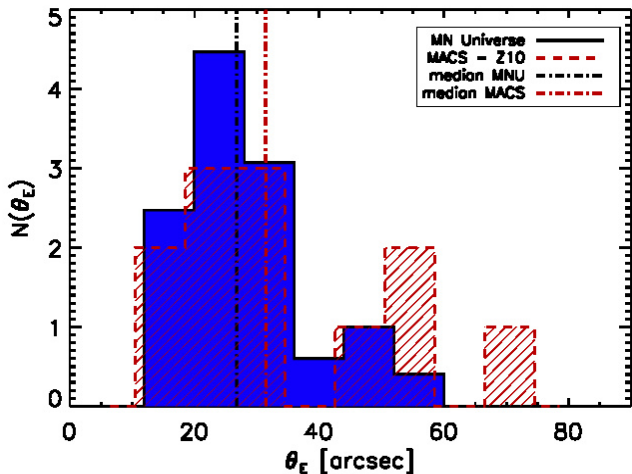
Projected enclosed mass in A2261 for different methods to get mass model (Coe et al. 2012)

Differences show mass-sheet degeneracy at work!



Einstein radius as function of source redshift in A 2261, obtained from different models (Coe et al. 2012)

# Too many too massive clusters?



Distribution of Einstein radii from MareNostrum simulations and from 12  $z > 0.5$  MACS clusters (Meneghetti et al. 2011)

Too large a discrepancy?

Also: high  $M_{\text{vir}}$  for high- $z$  clusters

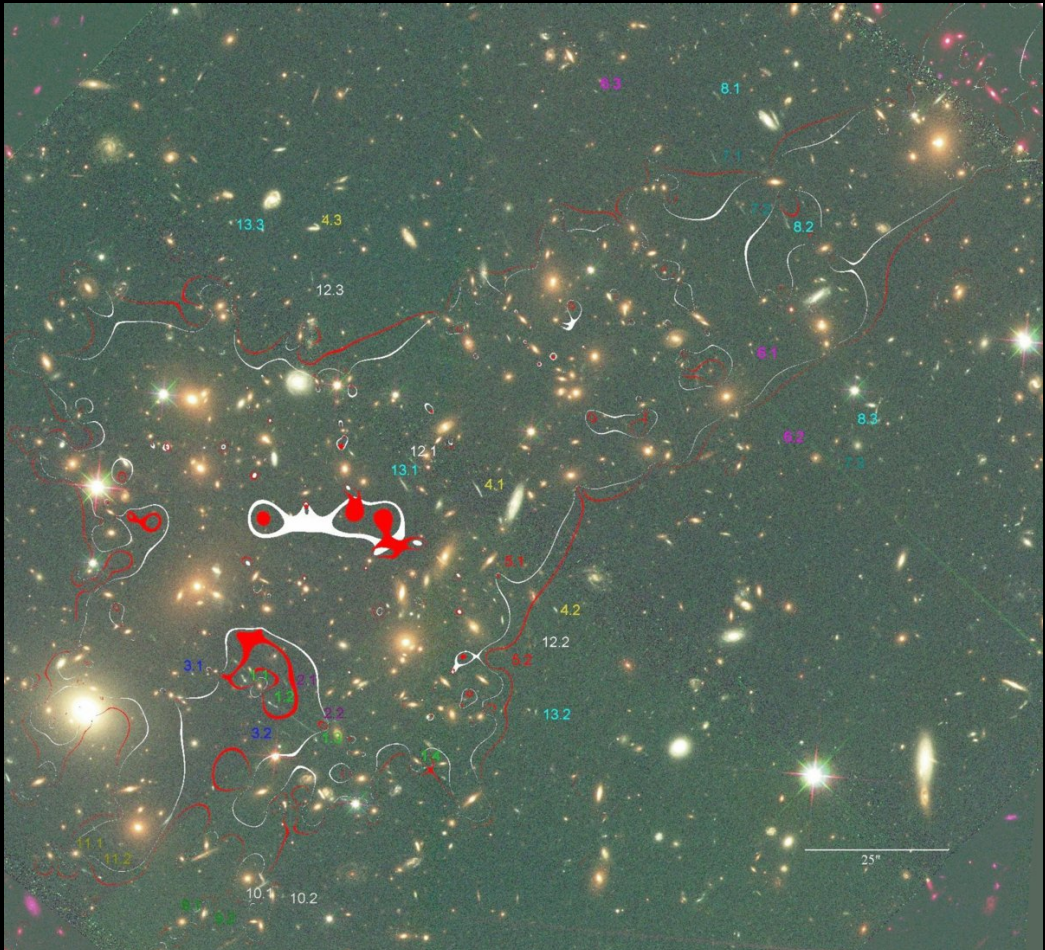
Arc statistics

# BUT

- Definition of ‘Einstein radius’ problematic

MACS J0717.5+3745  
( $z = 0.546$ )  
critical curves  
for  $z_s \sim 2.5$

Zitrin et al. (2009)

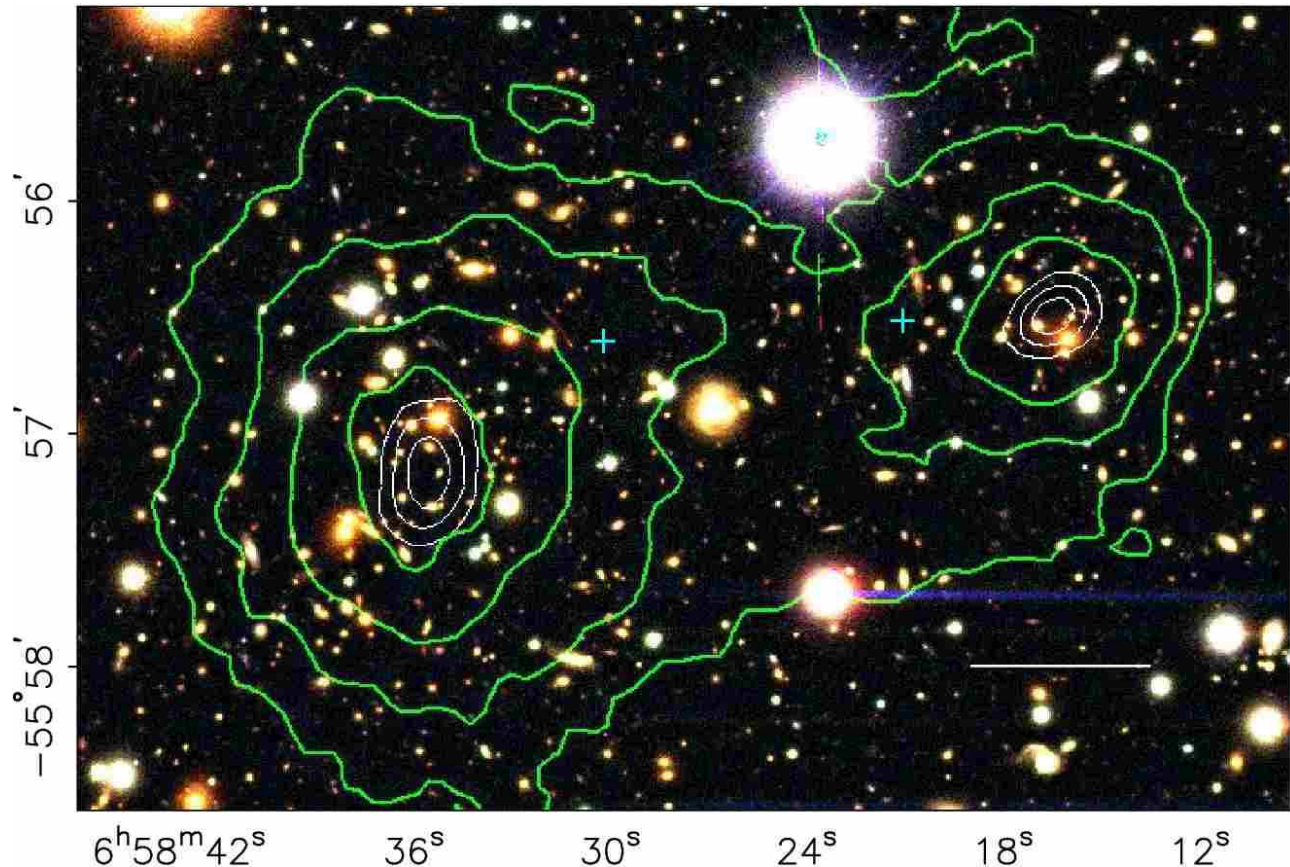


# BUT

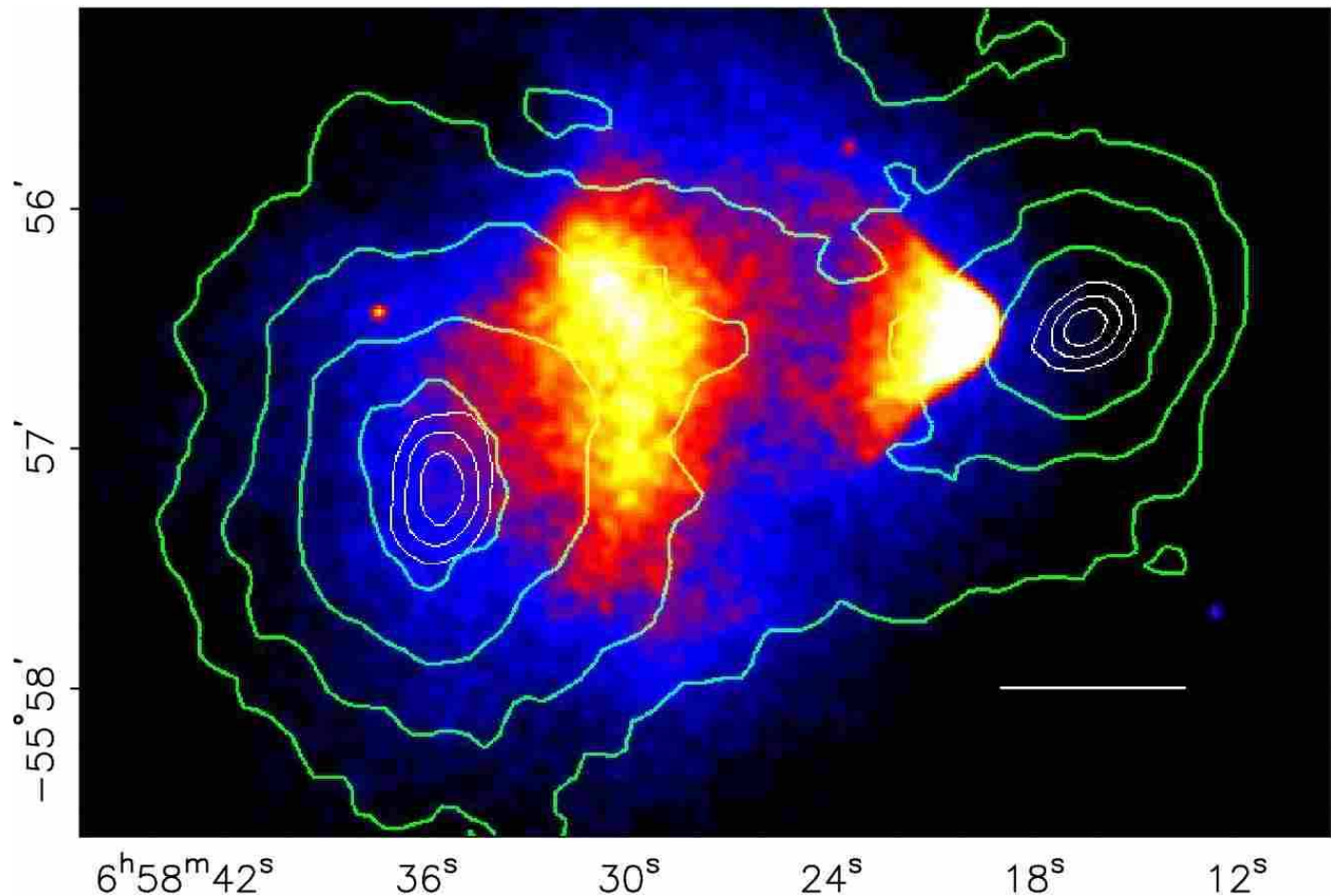
- Definition of ‘Einstein radius’ problematic
- Line-of-sight matter density (random projections) can strongly enhance lensing strength
- Strong lensing of clusters (significantly) affected by baryonic matter
- Selection bias – projection of triaxial or strongly asymmetric clusters
- Often, too few redshifts of strongly lensed sources known (in particular critical for high- $z$  clusters)
- Do we really know the ‘mass’-spectrum at the extreme end?
- How to properly compare observations with model predictions (*a posteriori* statistics)?

## Clusters are dominated by collisionless matter:

The Bullet Cluster is a pair of colliding galaxy clusters (Clowe et al. 2006)

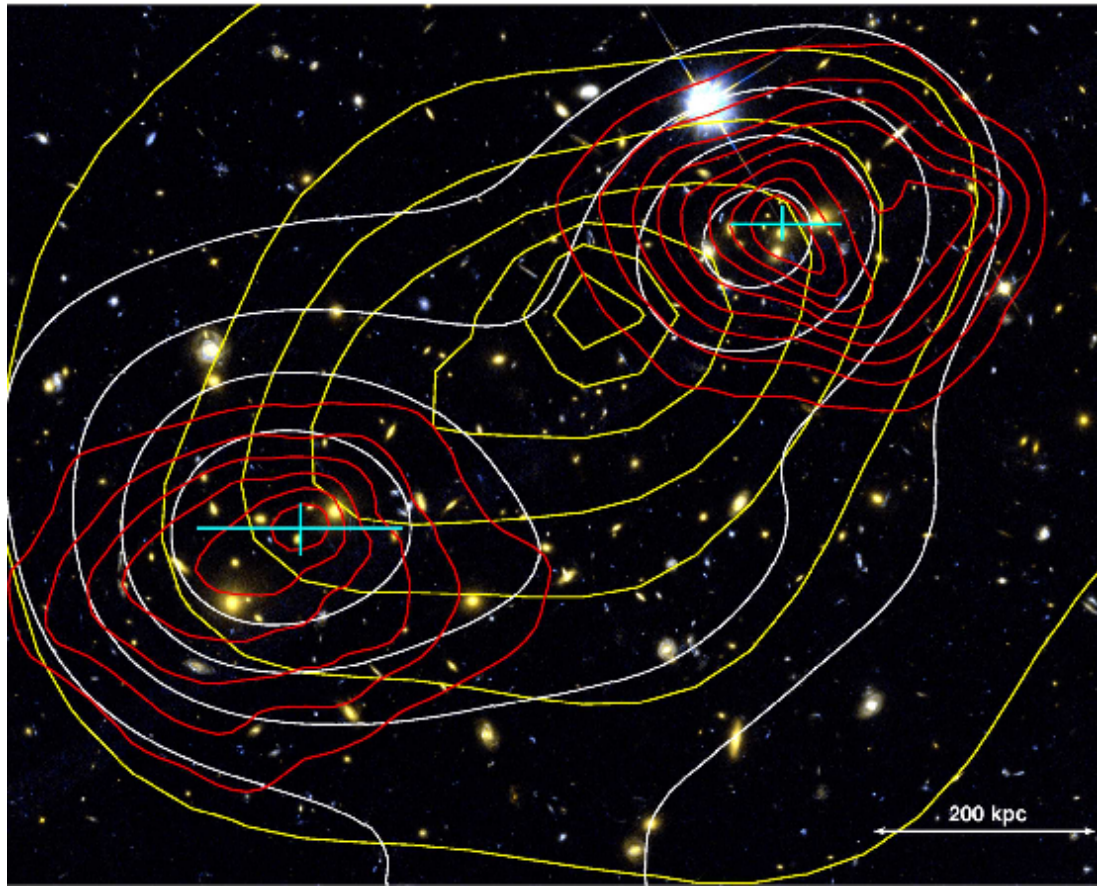


X-ray emission from the bullet cluster



- Lensing shows that most of the mass is located near the galaxies,
- and not centered on the gas, which is displaced by the collision.
- $\Rightarrow$  Most of the mass in this cluster pair must behave collisionless, like galaxies.
- Most of the mass is dark matter – the bullet cluster can not be explained by changing the law of gravity without invoking collisionless dark matter.
- The bullet cluster is not the only case where this clear distinction can be made...

## The cluster MACS J0025.4–1222 ( $z = 0.59$ )

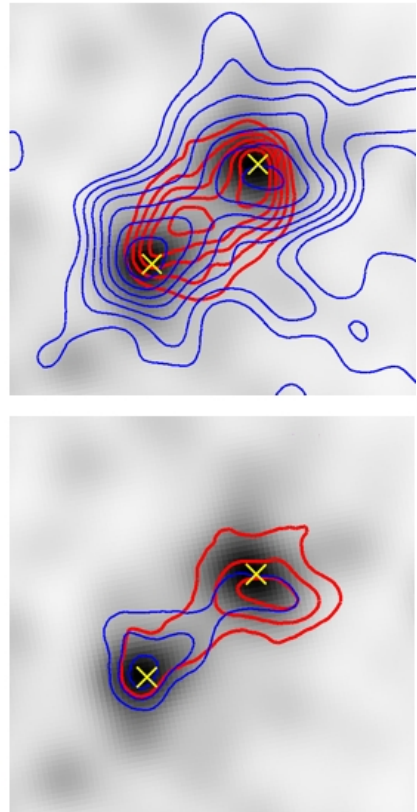
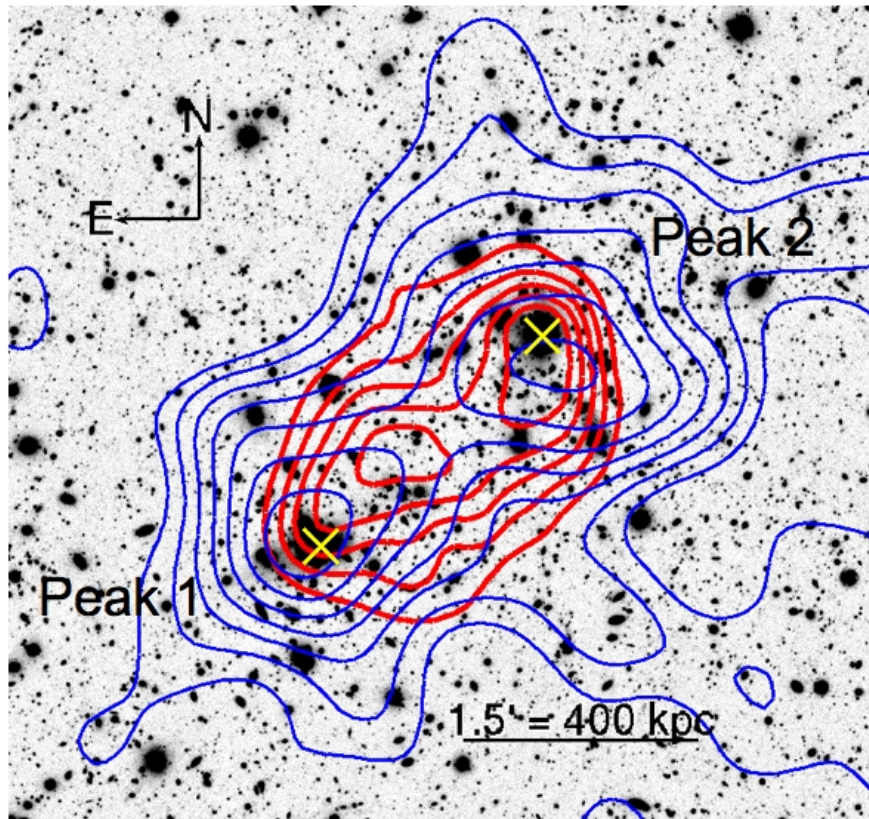


(Bradac et al. 2008)

red:  
surface mass density;

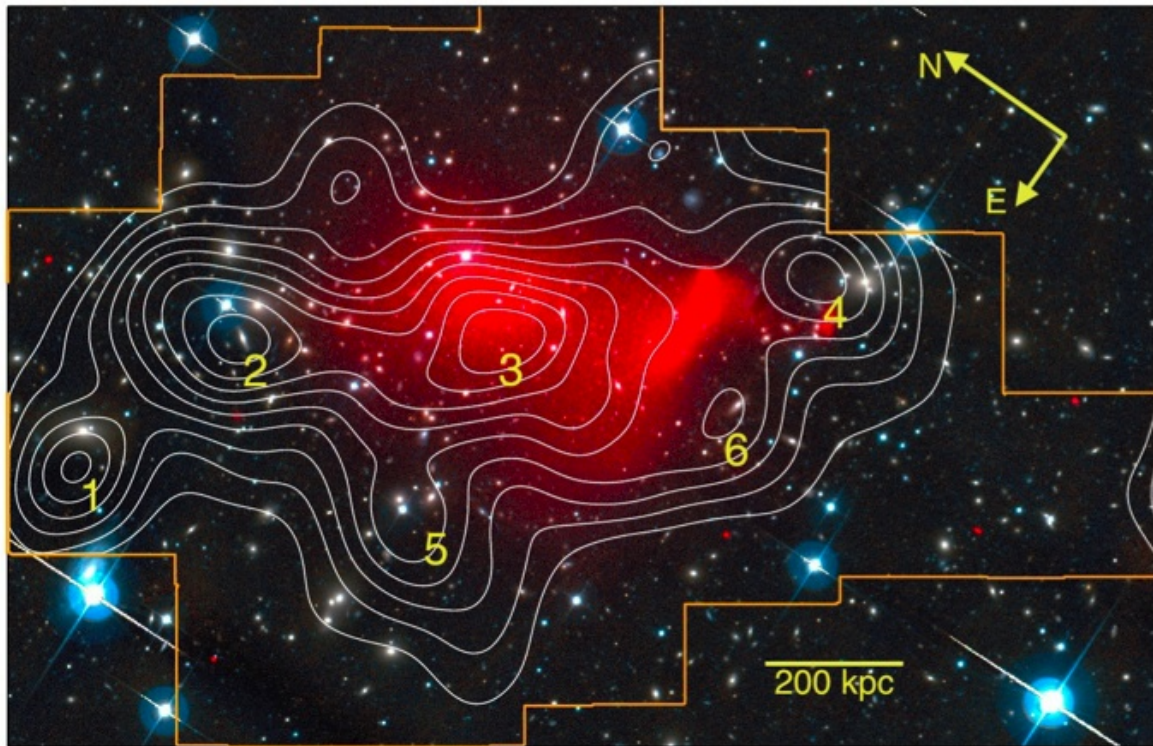
yellow:  
X-ray emission;

white:  
smoothed optical  
light.



A1758N (Ragazzine & Clowe 2011)

Blue: mass reconstruction; red: X-ray emission

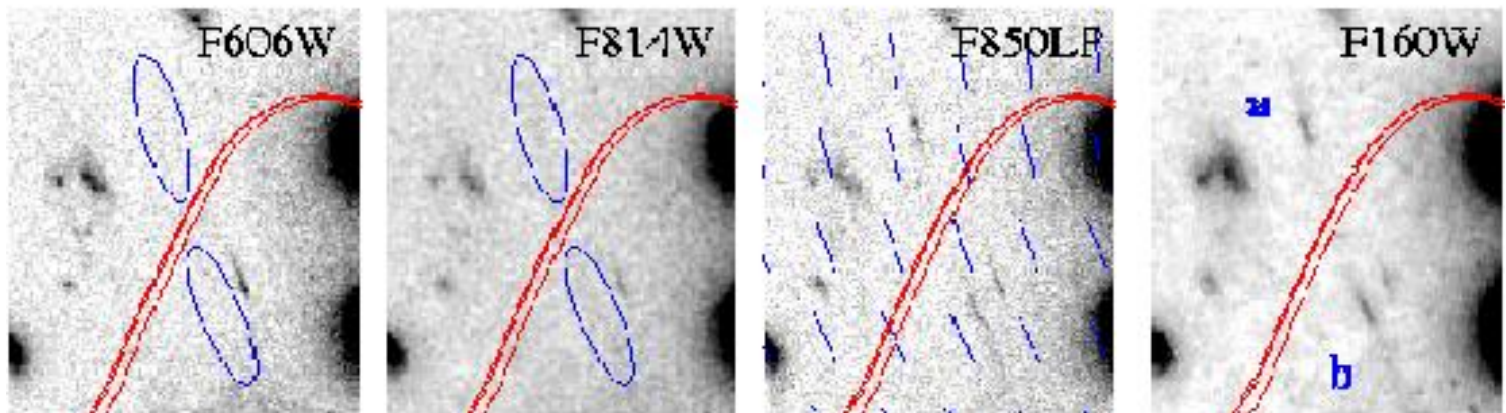


Jee et al. (2012): Abell 520 shows complicated structure in mass (contours) and X-ray emission (red shades)

# Natural telescopes

- Central region of strong lensing clusters yield high magnification
- There, fainter sources than elsewhere can be observed (and systematically searched for)

E.g.:  $z \sim 7$  galaxy behind A2218 (Kneib et al. 2004)



Without magnification, this galaxy would be too faint to be seen.

- Now a standard method to peek into the faint-end tail of source populations.

# Magnification bias at its best

A randomly located source has probability density  $p(\mu)$  for being magnified by  $\mu$ ;  $p(\mu)$  depends on: mass distribution in the Universe, source redshift, source size; for small sources,  $p(\mu) \propto \mu^{-3}$  at large  $\mu$ .

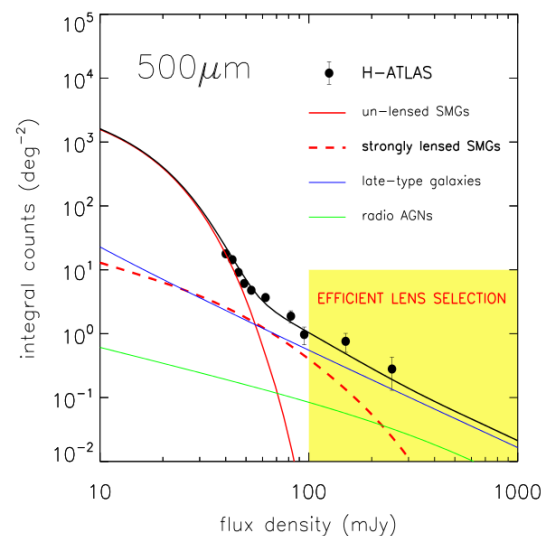
Observed source counts:

$$n(> S) = \int d\mu p(\mu) \frac{1}{\mu} n_0 \left( > \frac{S}{\mu} \right).$$

If  $n_0(> S)$  cuts off for  $S > S_{\max}$ , there still can be observed sources, i.e.,  $n(> S) > 0$  for  $S > S_{\max}$ .

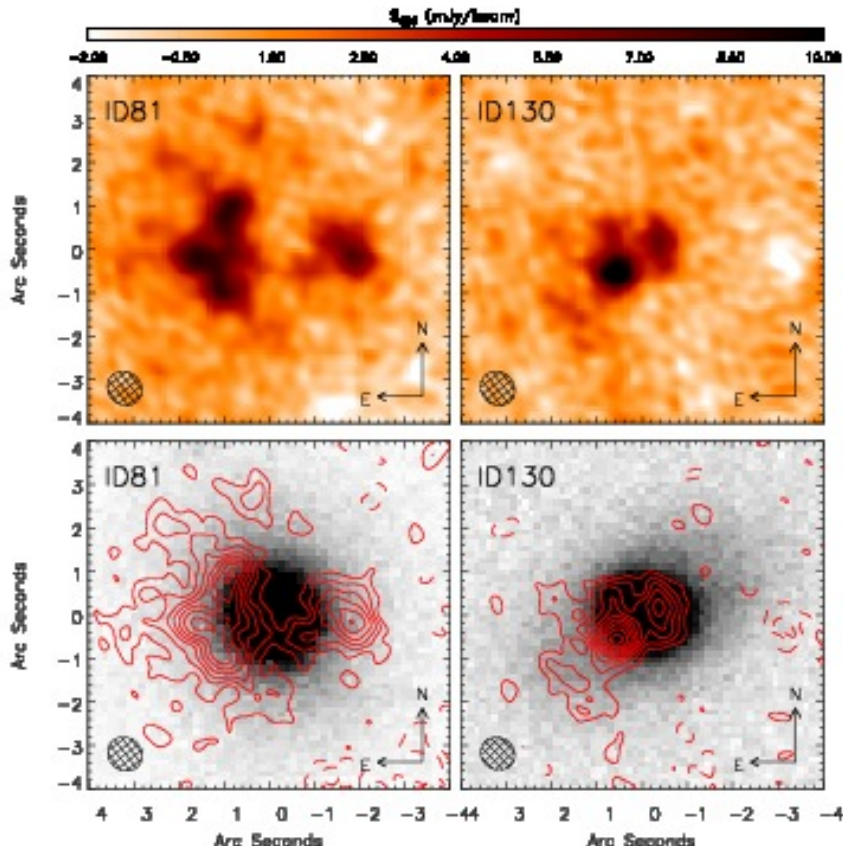
For  $S \gg S_{\max}$ , source counts can be dominated by lensed, highly magnified sources!

True for all population with Schechter-like luminosity function, best observable for population where  $n_0(S_{\max})$  is high.



Negrello et al. (2010)

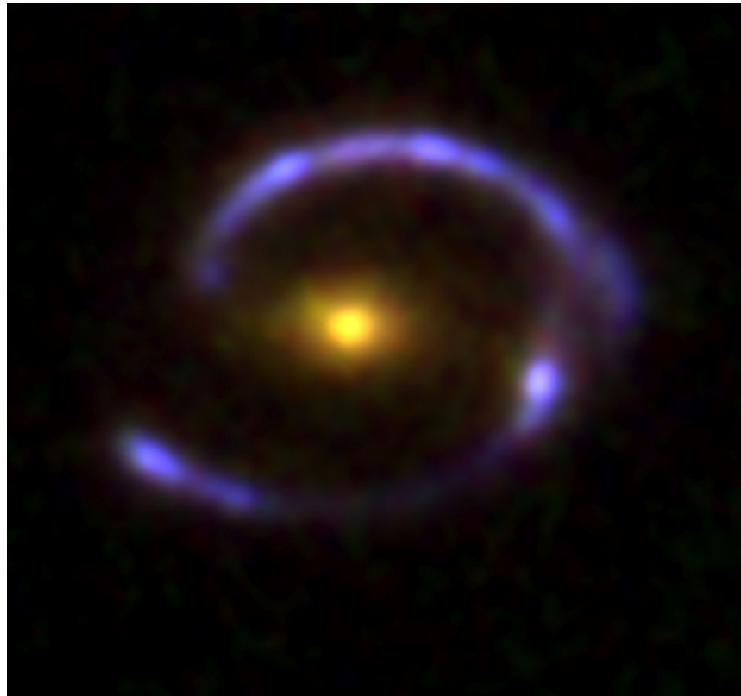
A large fraction of sub-mm sources are highly magnified distant galaxies



High-resolution imaging confirms lensing nature

Negrello et al. (2010)

The apparently most luminous sources of a population have high probability of being lensed!

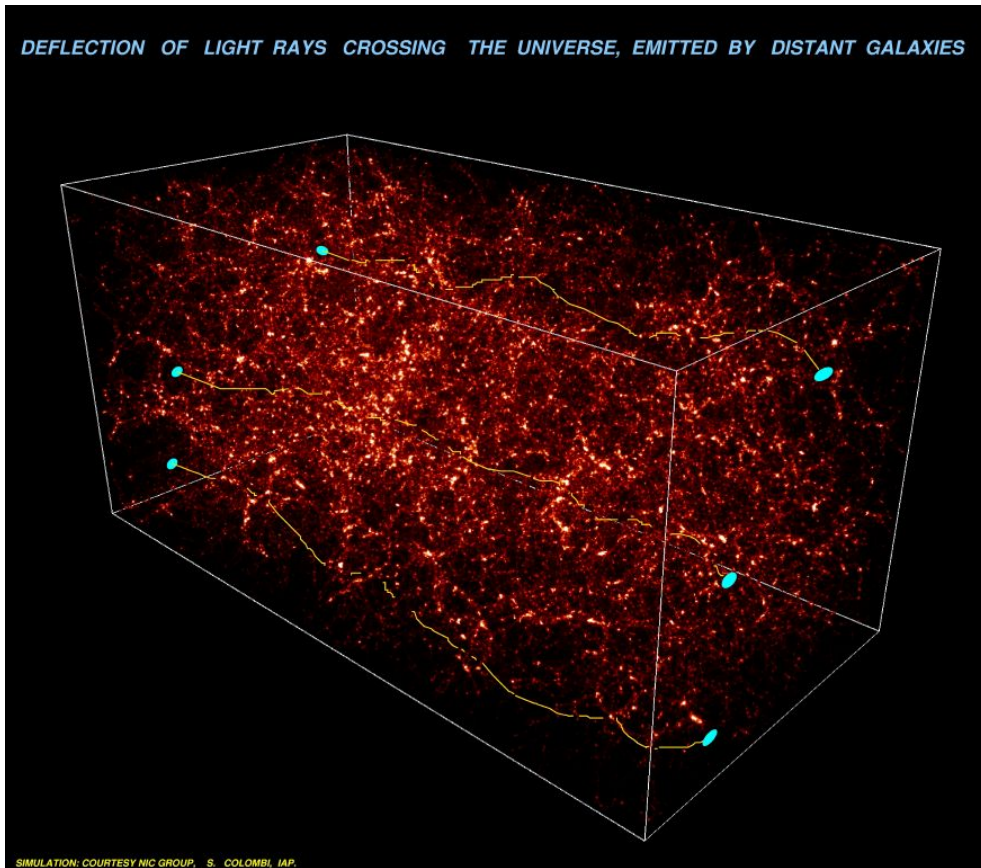


### Examples:

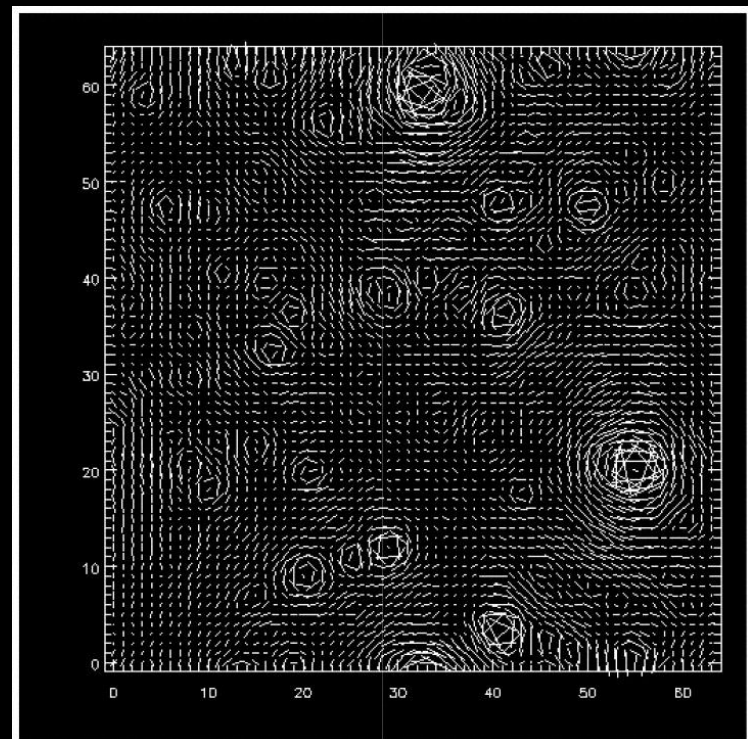
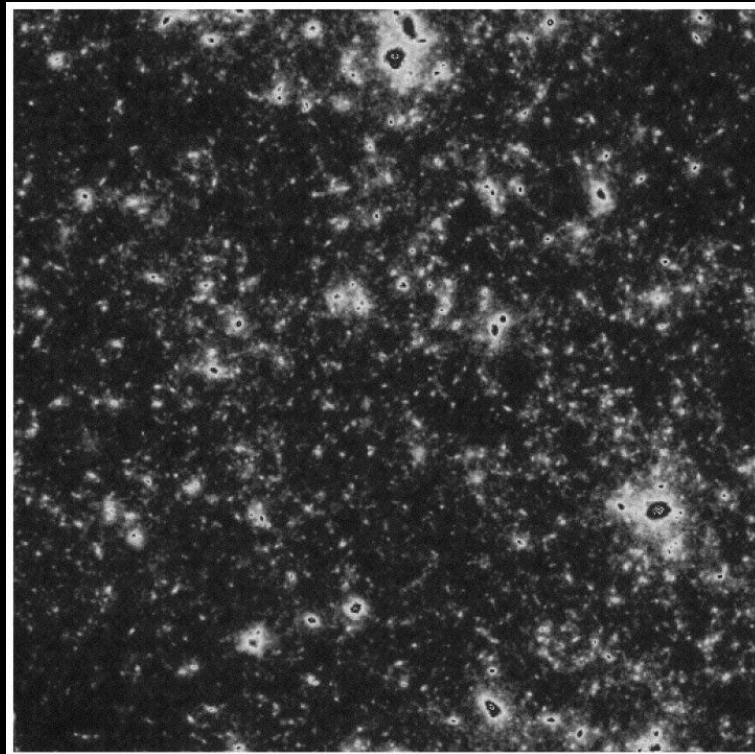
- F10214: The most luminous IRAS galaxy (at  $z \sim 2.2$ ; Broadhurst & Lehàr 1995);
- the extremely luminous  $z = 3.87$  quasar APM 08279+5255 (Irwin et al. 1998)
- the  $m_B \lesssim 21$ ,  $z \sim 3$  Lyman-break galaxies cB58, Cosmic Eye, and 8 o'clock arc

Due to high sky density, and the fact that strong negative K-correction causes observed flux at  $L^*(z)$  almost independent of redshift, (sub-)mm galaxies are most strongly affected by this magnification bias.

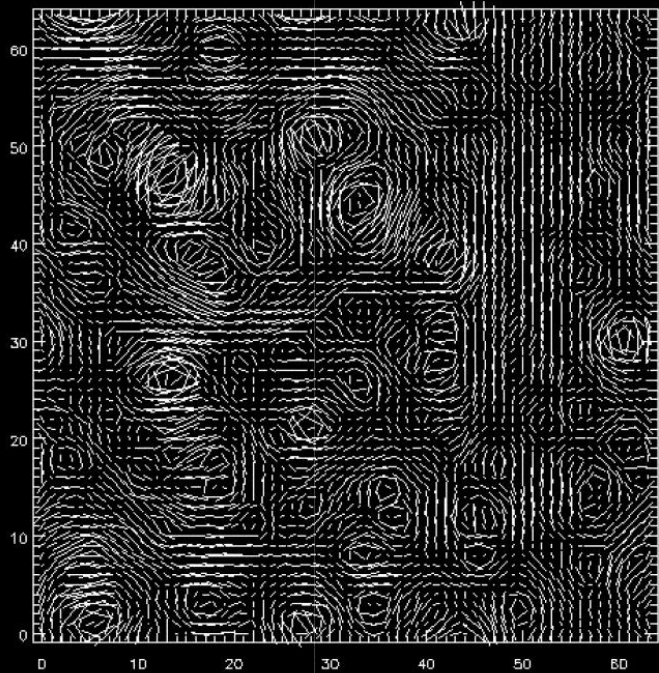
# Cosmic shear = lensing by the LSS



# Mass-shear relation



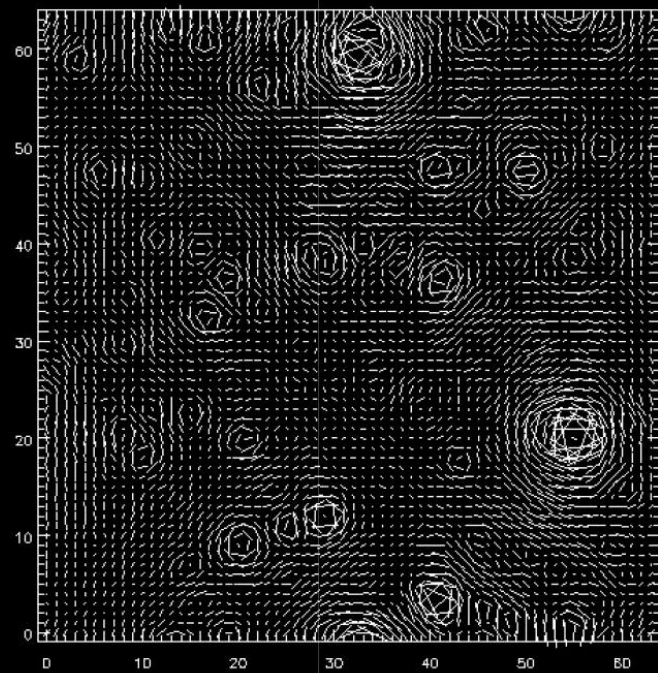
Projected mass distribution of the LSS (left) and shear field (right; from Jain et al 2000). Mass concentrations correspond to circular patterns of tangentially oriented shears.



high-density Universe

$$\Omega_m = 1$$

from Jain, Seljak & White 2000



low-density Universe

$$\Omega_m = 0.3$$

Lensing properties of 3-D mass distribution determined by ( $z$ -weighted) l.o.s. projection of density contrast, symbolically:

$$\kappa(\boldsymbol{\theta}) = \int dz w_\kappa(z) \delta(D\boldsymbol{\theta}, z) .$$

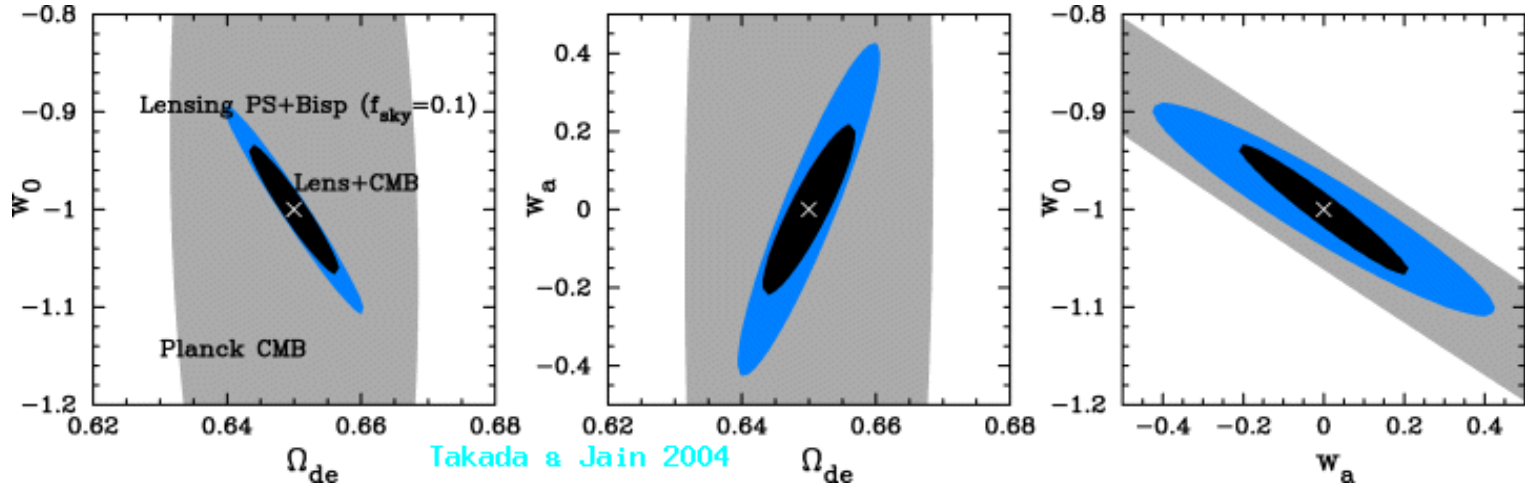
Second-order statistical properties of  $\kappa$  described by its power spectrum, which is l.o.s. integrated 3-D power spectrum,

$$P_\kappa(\ell) = \int dz w_P(z) P(\ell/D, z) .$$

Shear correlation function – measured by ellipticity correlation – probes  $P_\kappa$  directly  
Different source redshift distributions yield different weight functions  $w_P$ , and thus  
different information on  $P(k, z)$ .

Note:  $P_\kappa$  depends on properties of 3-D mass distribution (through  $P(k, z)$ ) and on  
geometry of the Universe, contained in  $w_P$ .

Cosmic shear is seen as one of the most promising tools for studying properties of Dark Energy:



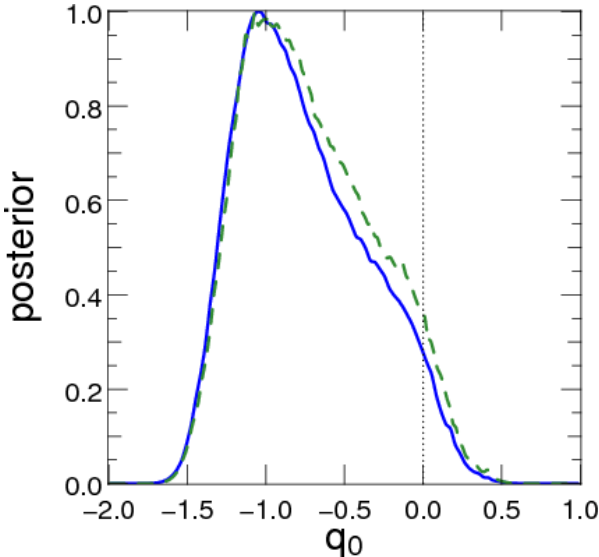
Accuracy increases with sky area, depth, photometric coverage (for redshift estimates), PSF quality and stability.

Many projects ongoing/planned for precision measurements of cosmic shear, e.g.:

KiDS/VIKING (1500 deg<sup>2</sup>, 9 bands, Paranal, start: 2011)

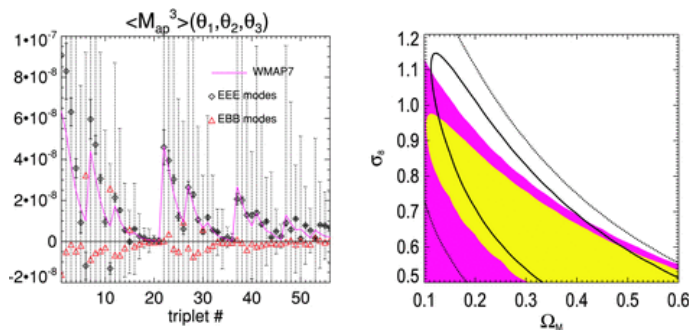
DES (5000 deg<sup>2</sup>, 5 bands, CTIO, start: 2012); HSC

EUCLID (14000 deg<sup>2</sup>, 4 bands – supplemented from ground, ESA, launch: 2020)

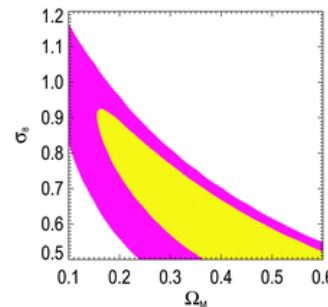


## State of the art

From HST-COSMOS survey, independent evidence for cosmic acceleration  
 (from  $\sim 1.5 \text{ deg}^2$  of HST imaging – COSMOS)  
 EUCLID will cover  $10^4$ -times the area !!!  
 Schrabback et al. (2010)



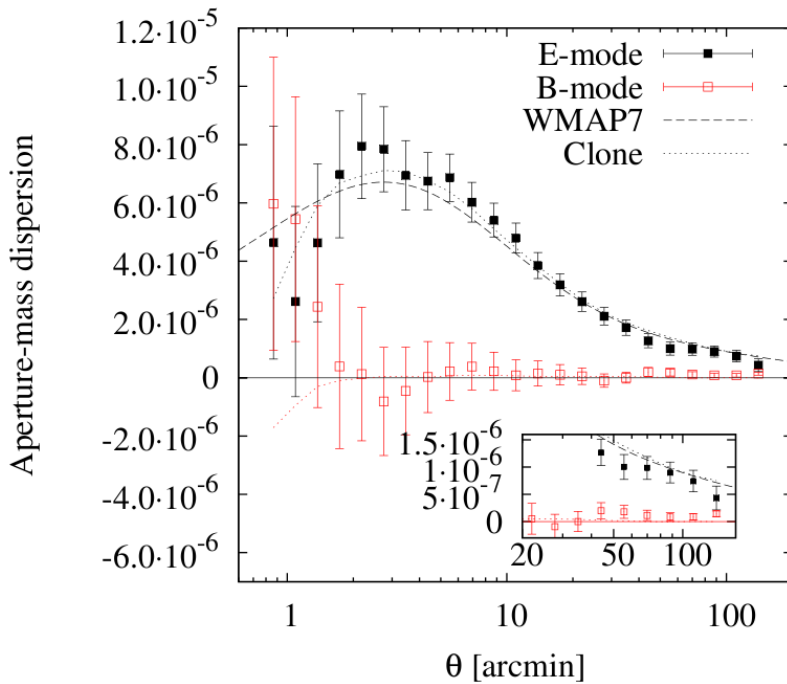
Semboloni et al. (2011)



Constraints from cosmic shear in  
 $\Omega_m - \sigma_8$ -plane  
 Here in combination with third-order cosmic shear measurements

# Results from CFHTLenS

154 deg<sup>2</sup> in five optical bands, taken with Megacam@CFHT;  
permits accurate photometric redshift information;  
very high imaging quality



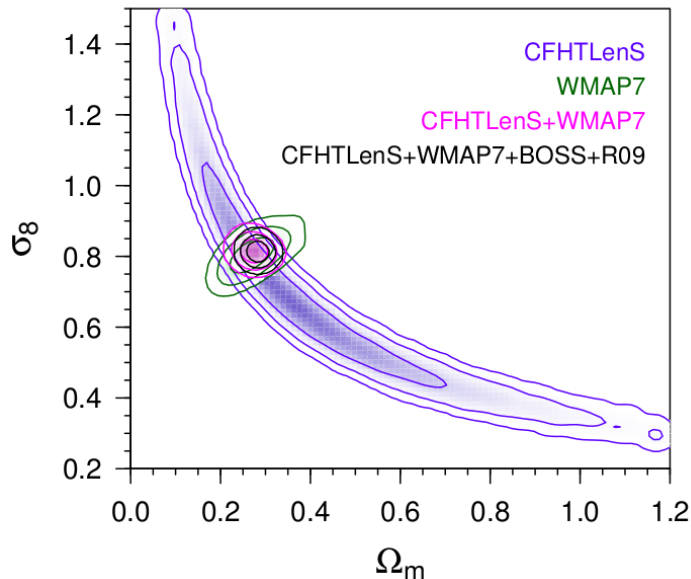
Cosmic shear signal from CFHTLenS, in form of aperture statistics

Curve shows expectation from WMAP7 cosmology

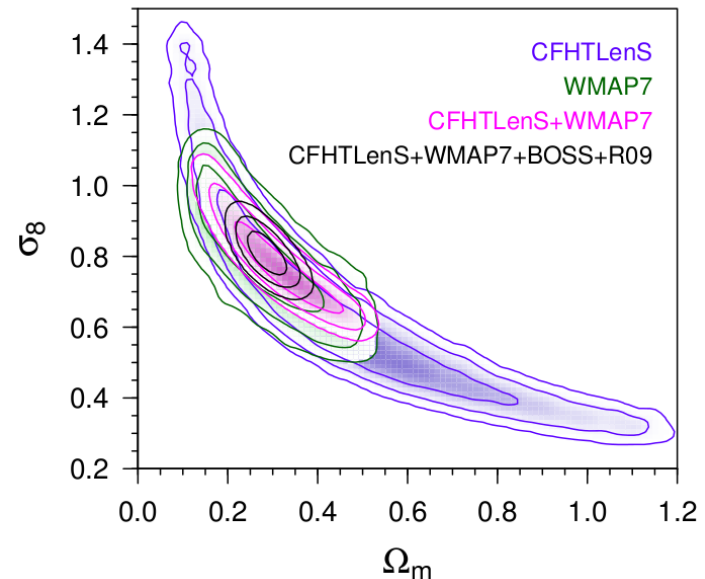
B-modes compatible with zero

(Kilbinger et al. 2013)

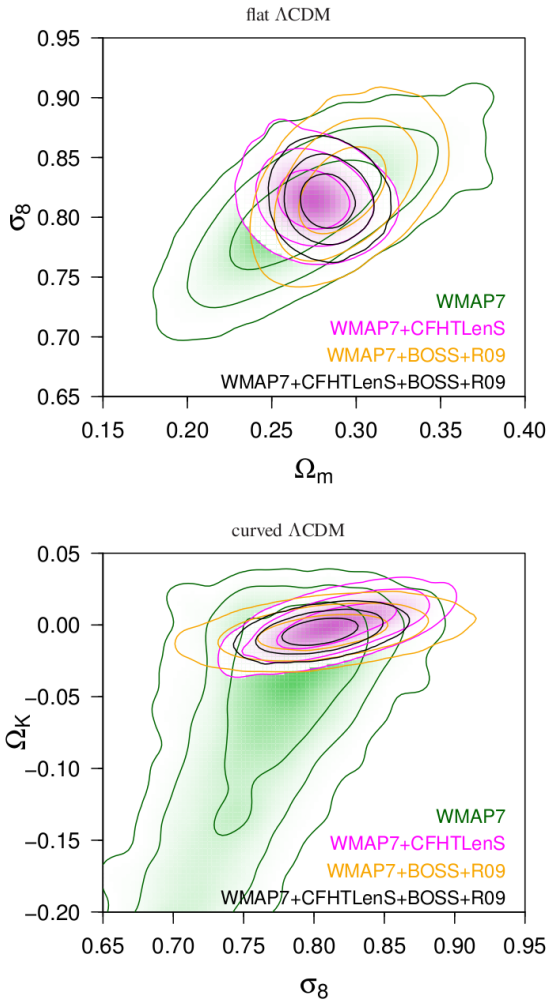
flat  $\Lambda$ CDM



flat  $w$ CDM



Marginalized posterior contours, from different data sets and their combination (Kilbinger et al. 2013).



Cosmic shear from CFHTLenS provides significant – and independent – constraints on parameters;

Results are fully compatible with flat  $\Lambda$ CDM:

- no indication for a more complicated e.o.s. of DE
- no indication for deviations from GR

$$\Omega_m = 0.283 \pm 0.010; \sigma_8 = 0.813 \pm 0.014$$

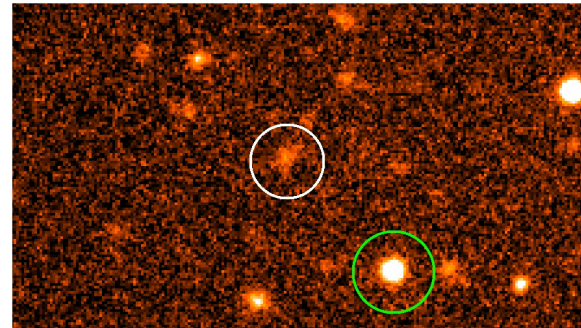
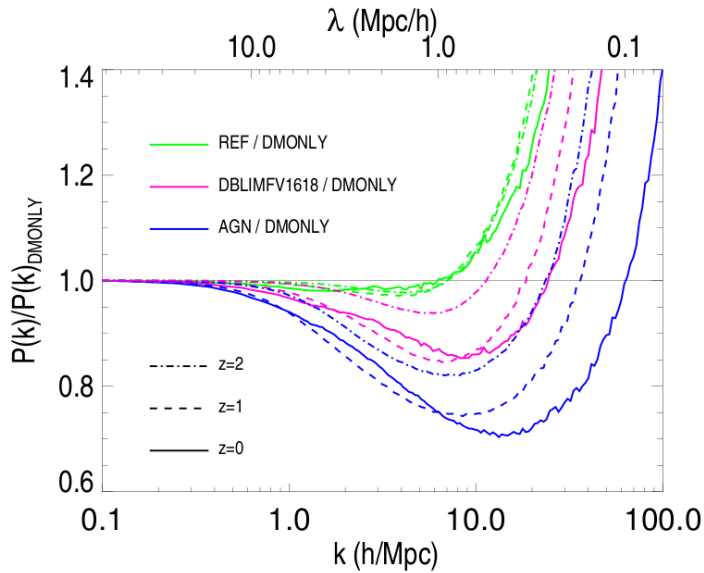
(Kilbinger et al. 2013)

# Issues

CS is **difficult** to measure quantitatively.

Community-wide effort to understand and improve shape measurement.

Several astrophysical effects can contaminate shear signal –



intrinsic alignments, selection bias, etc.:  
Need to be properly accounted for!

Theoretical predictions need to be improved (e.g., influence of baryons on power spectrum)

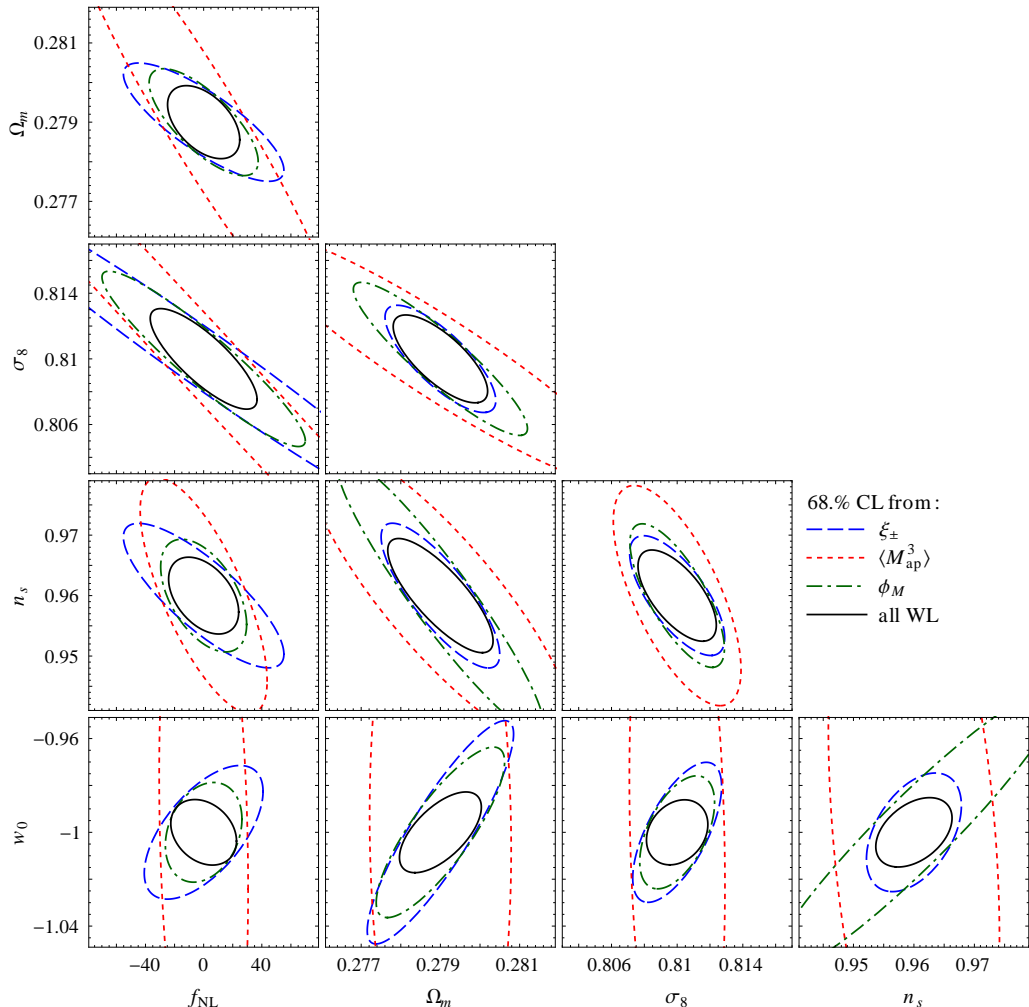
from Sembolini et al. (2011) based on OWL simulations.

# Extensions

Statistics beyond second order (e.g., shear 2PCFs) contain essential additional information, not yet included in most forecasts;

these include: third-order shear statistics, shear peak abundance, shear peak correlation functions and profiles;

(Hilbert et al. 2012)



# Galaxy-galaxy lensing and bias

Galaxies (and groups and clusters) are expected to **approximately** trace underlying matter distribution, though with some bias  $b$  and non-perfect spatial correlation coefficient  $r$ ,

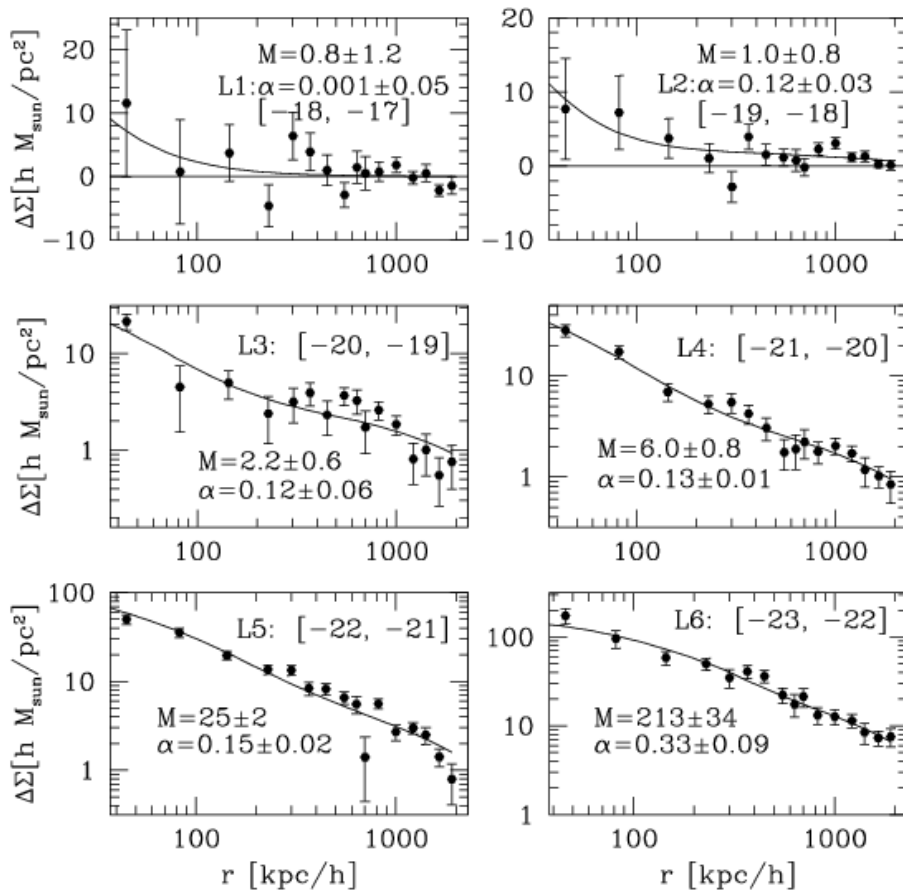
$$P_{\text{gg}}(k, z) =: b^2 P_{\text{mm}}(k, z) ; \quad P_{\text{gm}}(k, z) =: b r P_{\text{mm}}(k, z) .$$

$b$  and  $r$  in general scale- and redshift-dependent, and depend on galaxy mass.

Both can be measured without additional assumptions from lensing:

1. The correlation between galaxy positions and shear,  $\langle \gamma \rangle(\theta)$ , measures directly the mean matter distribution associated with galaxies (**galaxy-galaxy lensing**);
2. Cosmic shear measures directly the matter density power spectrum;
3. Galaxy correlation function is linearly related to  $P_{\text{gg}}$ .

From measuring all three of these,  $b$  and  $r$  can be determined directly.

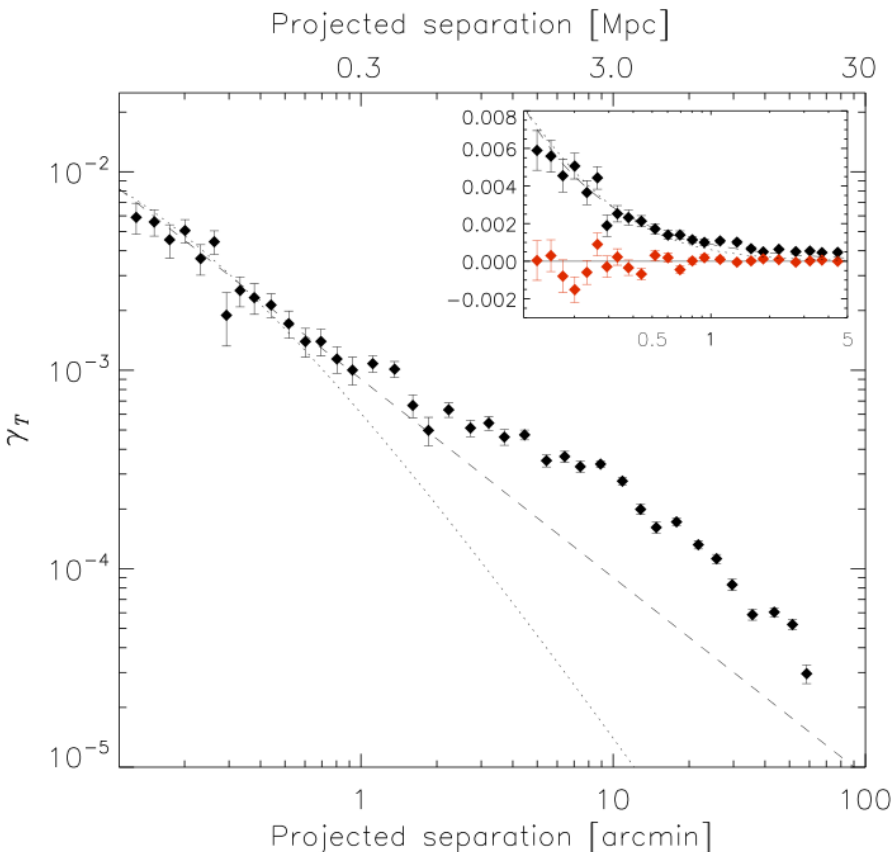


Galaxy-galaxy lensing from the SDSS;

signal shown in different luminosity bins of galaxies;

curves are fits from the halo model.

Figure from Seljak et al. (2004);

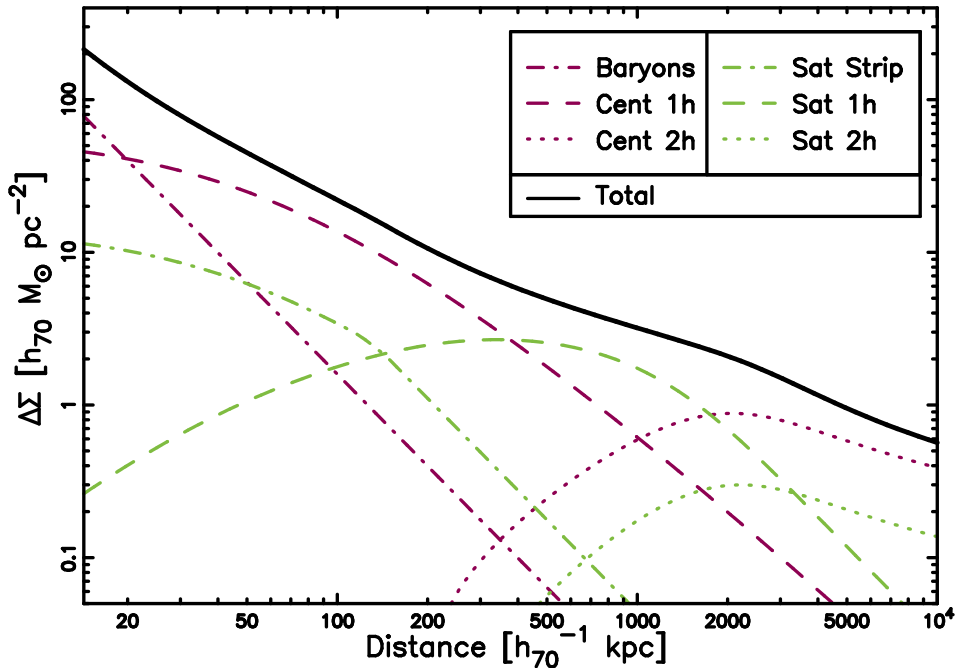


Tangential shear profile around ‘bright’ galaxies in the RCS2 survey (van Uitert et al. 2011)

For small separations, profile well fitted by either SIS or NFW profile;

for large separations, signal clearly exceeds these simple models:

the mass correlated with galaxies extends much further than the dark matter halo in which the galaxy is embedded – galaxies and mass are correlated at large separations.



$$\Delta\Sigma_{\text{cent}} = \Delta\Sigma_{\text{cent}}^{1h} + \Delta\Sigma_{\text{cent}}^{2h}$$

$$\Delta\Sigma_{\text{sat}} = \Delta\Sigma_{\text{sat}}^{\text{strip}} + \Delta\Sigma_{\text{sat}}^{1h} + \Delta\Sigma_{\text{sat}}^{2h}$$

$$\Delta\Sigma = \Delta\Sigma_{\text{bar}} + (1 - \alpha)\Delta\Sigma_{\text{cent}} + \alpha\Delta\Sigma_{\text{sat}}$$

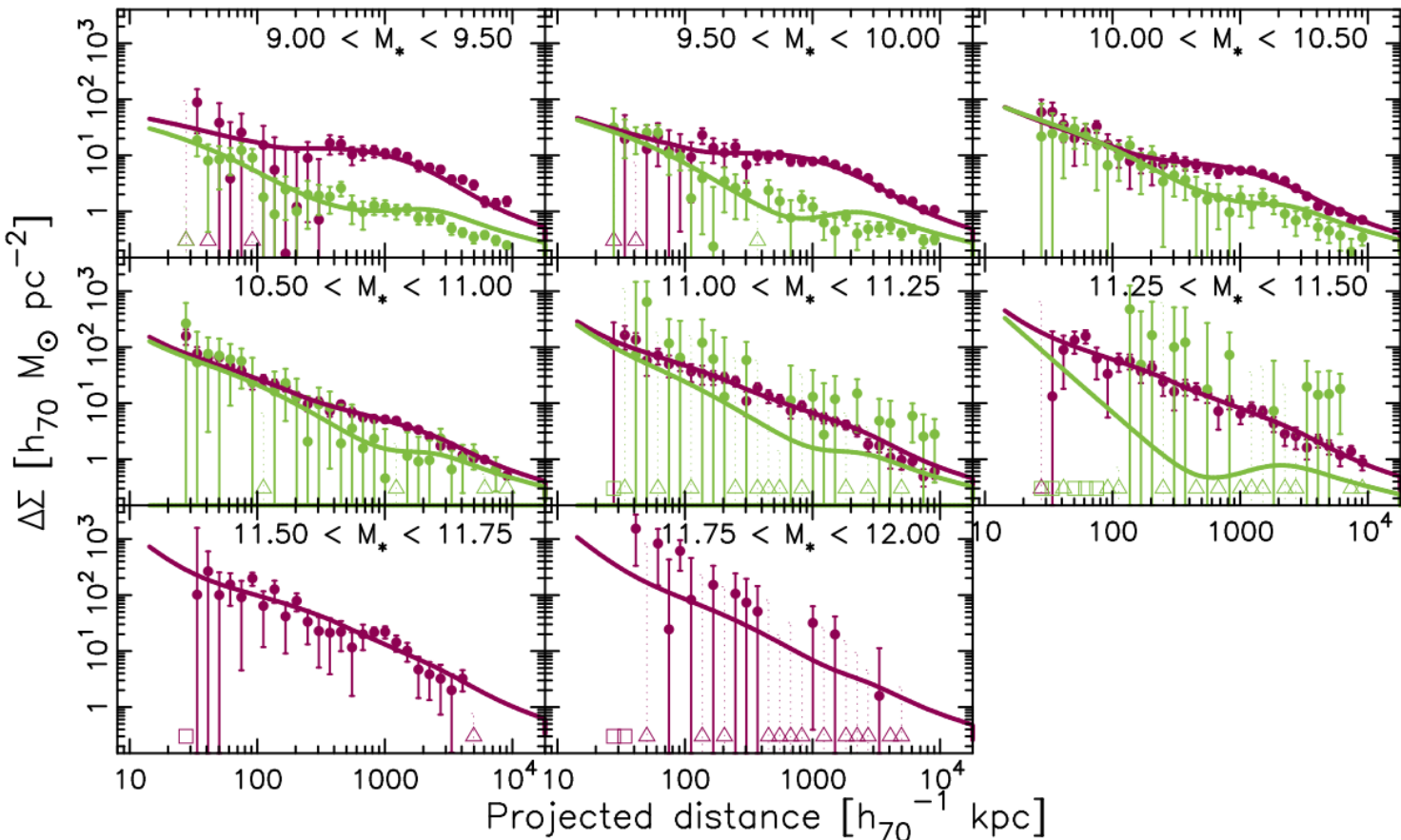
GGL results are often interpreted in terms of halo model, illustrated here:

$$M_{200} = 10^{12} M_{\odot};$$

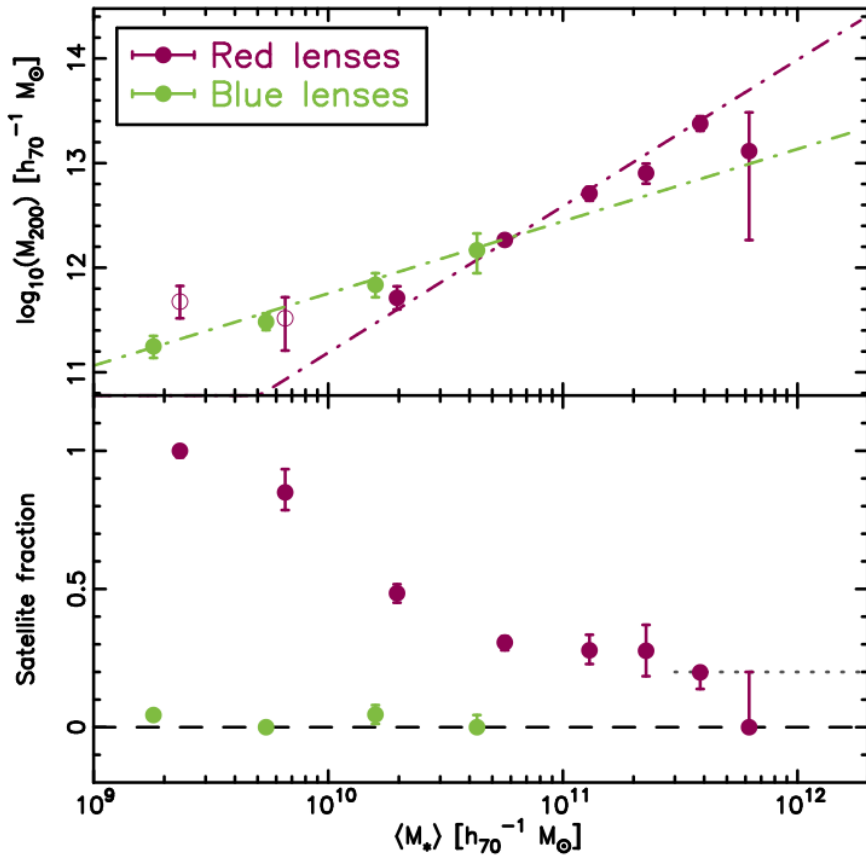
$$M_* = 5 \times 10^{10} M_{\odot};$$

$$\text{satellite fraction } \alpha = 0.2$$

from Velander et al. (2013)



GGL results from the CFHTLenS survey; for early- and late-type galaxies separately, for different stellar-mass bins (Velander et al. 2013)



Relation between stellar mass and mean halo mass (top) and satellite fraction  $\alpha$  as function of stellar mass (bottom),

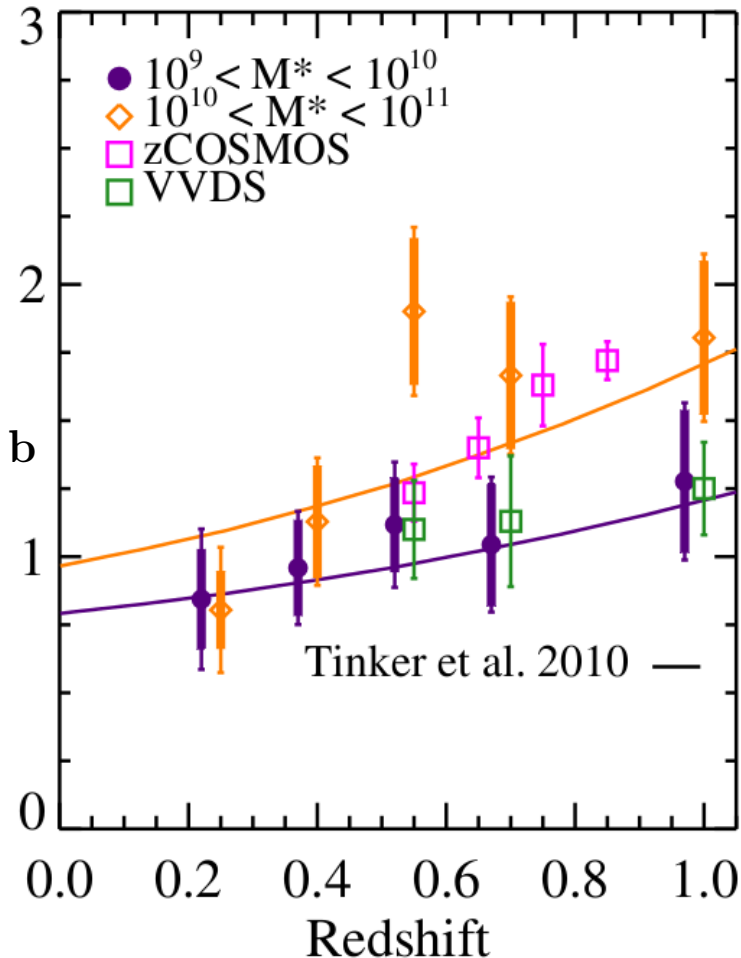
for early- (purple) and late-type (green) galaxies

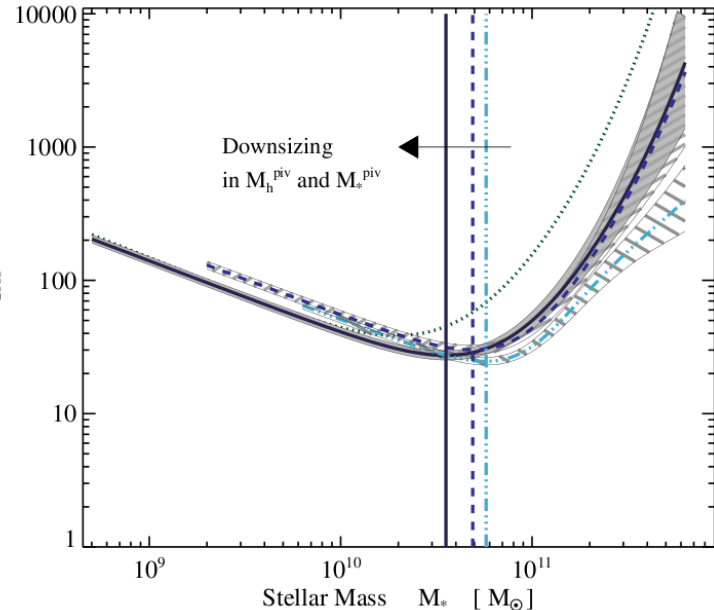
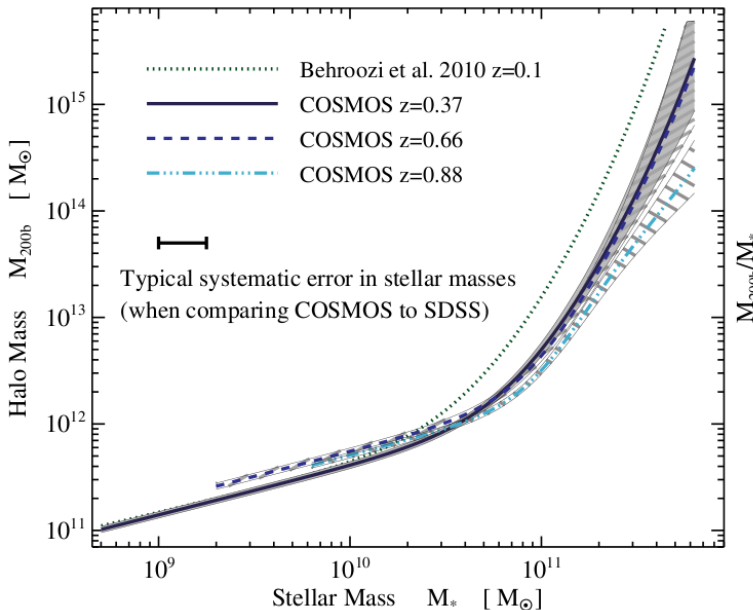
almost all late-type galaxies are centrals, the satellite fraction of early-type galaxies strongly depends on galaxy mass (or luminosity)

Velander et al. (2013)

Results from COSMOS survey (Jullo et al. 2012)

- Bias of galaxies increases with redshift
- Bias increases with stellar mass of galaxies
- Correlation coefficient  $r \approx 1$  (though with large error bars): no evidence for stochasticity of bias





Combining galaxy correlations and galaxy-galaxy lensing in the framework of the halo model, the relation between stellar mass and dark matter halo mass can be derived from COSMOS survey (Leauthaud et al. 2012)

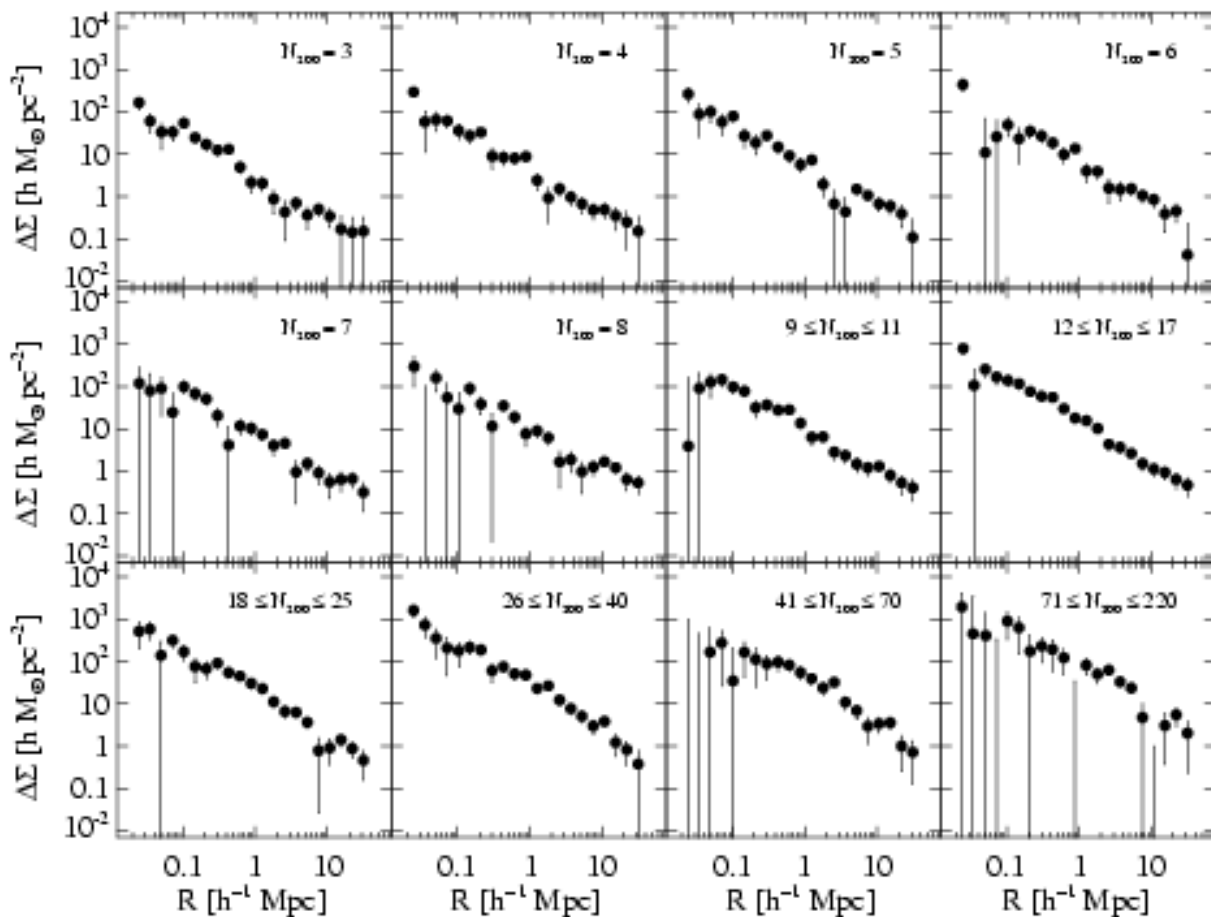
A clearly preferred scale for most efficient transformation of stars into gas.

## Cluster-shear correlations

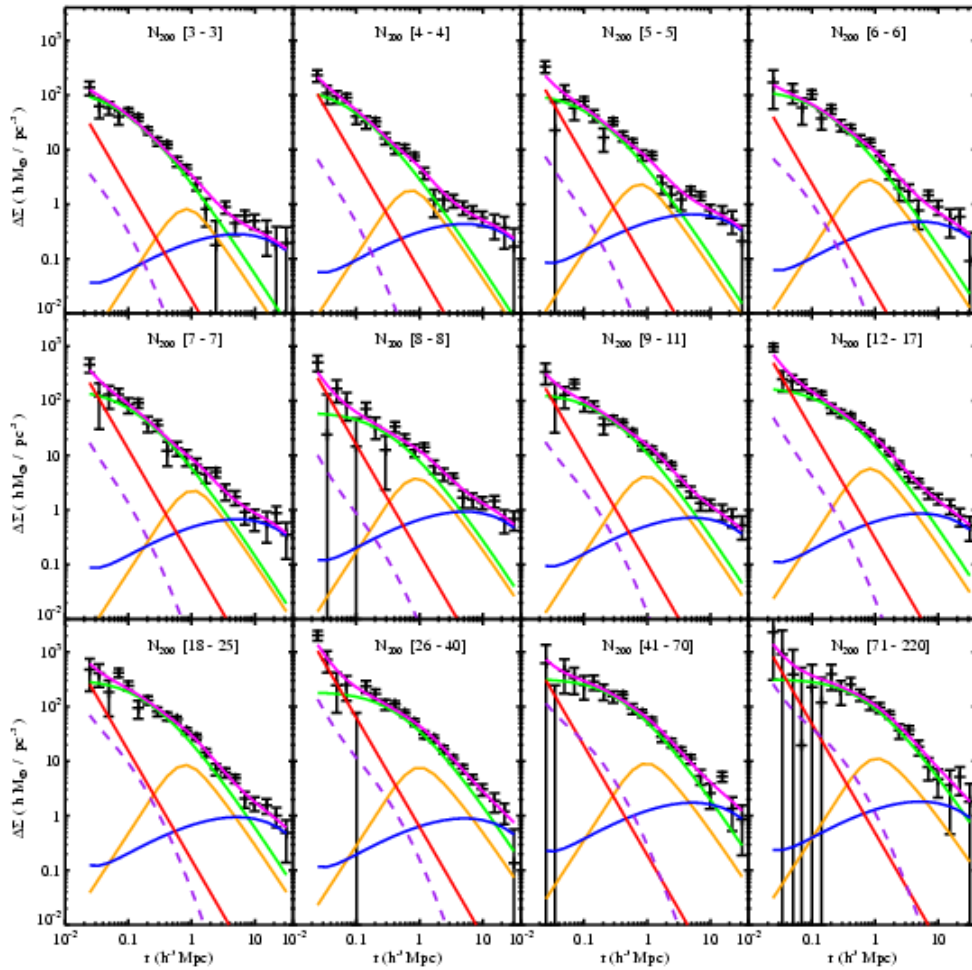
Idea: Weak lensing signal of many clusters are superposed to get average mass profile;

clusters can be binned according to richness, luminosity, ...

Recent results were presented in a series of papers from SDSS collaboration, with very high significance



from Sheldon et al. (2007); note that shear signal is measured out to  $> 20h^{-1} \text{ Mpc}$



NFW fit

miscentered halos (orange)

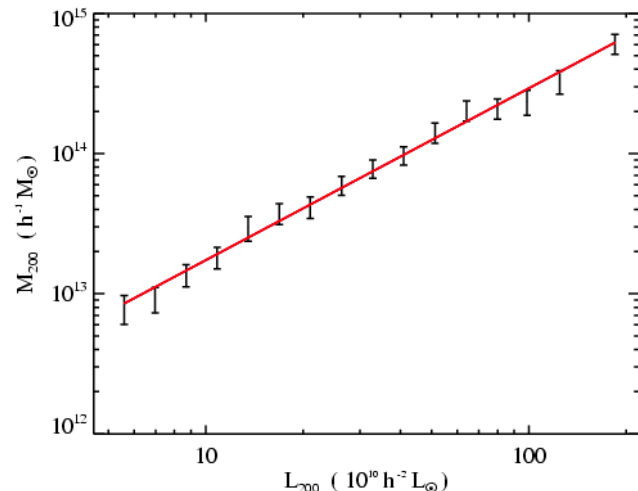
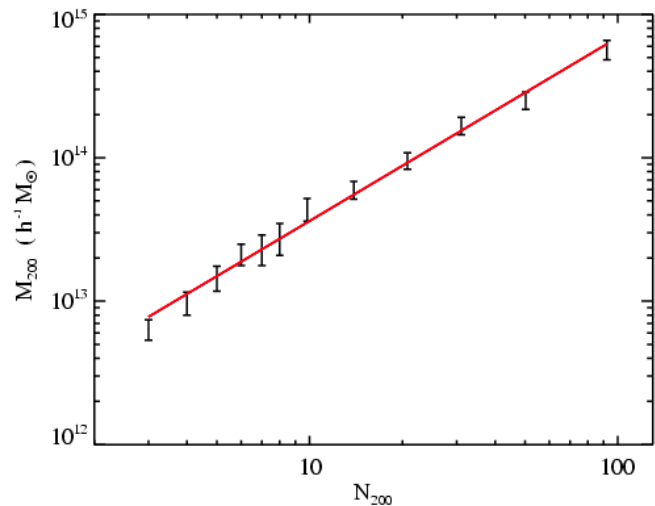
BCG

neighboring halos

non-linear shear (purple)

Sum

the binning can also be performed in luminosity from Johnston et al. (2007)



Results:

mass-richness (left) and mass-luminosity (right) relation, obtained by fitting NFW-profiles plus corrections to weak lensing signal in richness and luminosity bins yields mass calibration for scaling relations of clusters  
from Johnston et al. (2007)

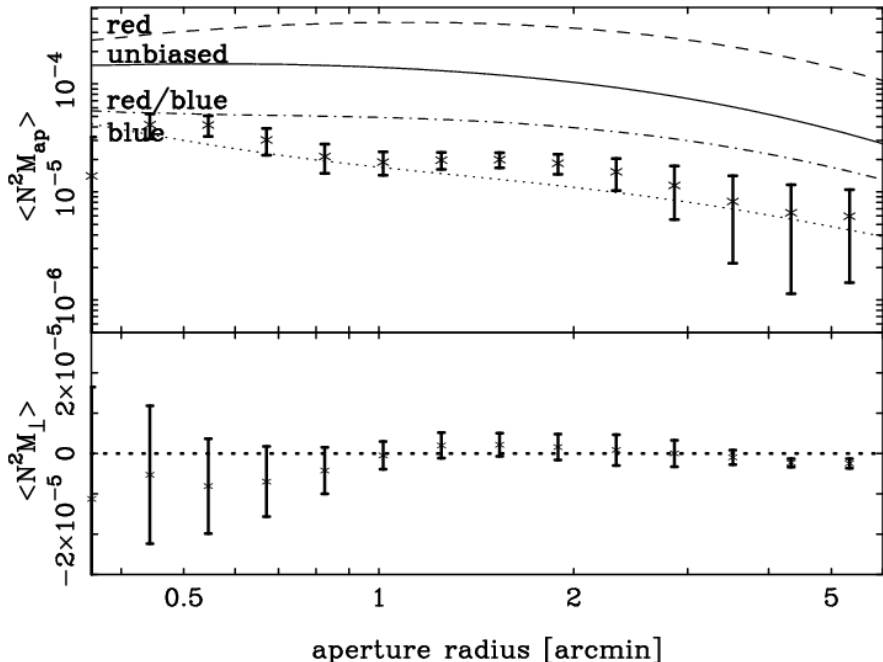
# Galaxy-galaxy-galaxy lensing

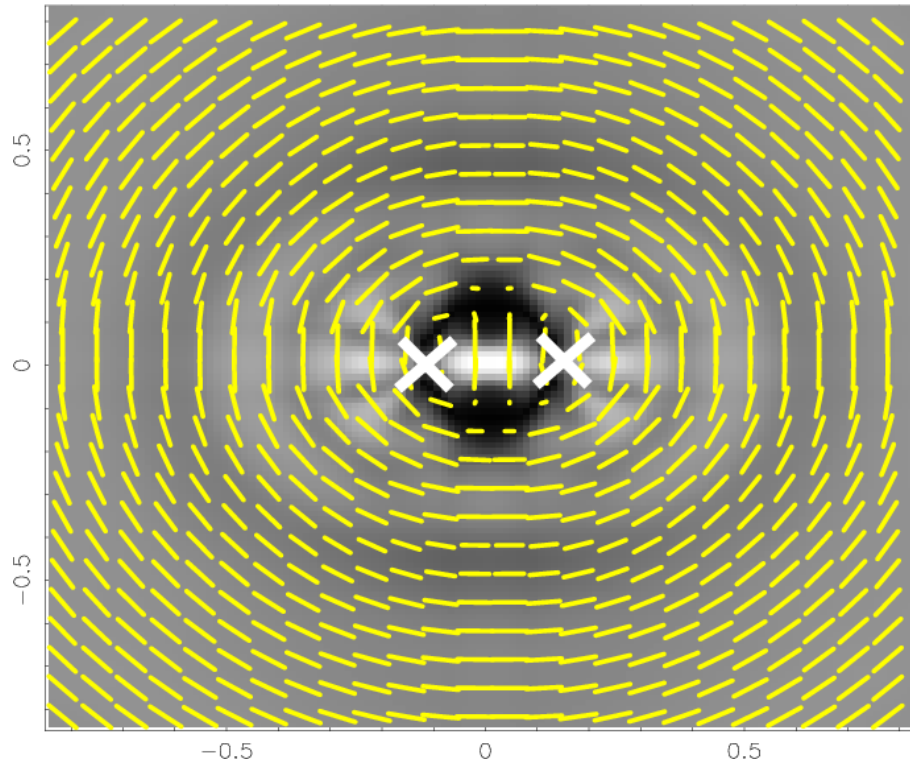
GGL measures correlation of galaxies with mass

One can correlate shear (i.e. mass) with **pairs** of galaxies and thus get the excess mass related to pairs – galaxy-galaxy-galaxy lensing

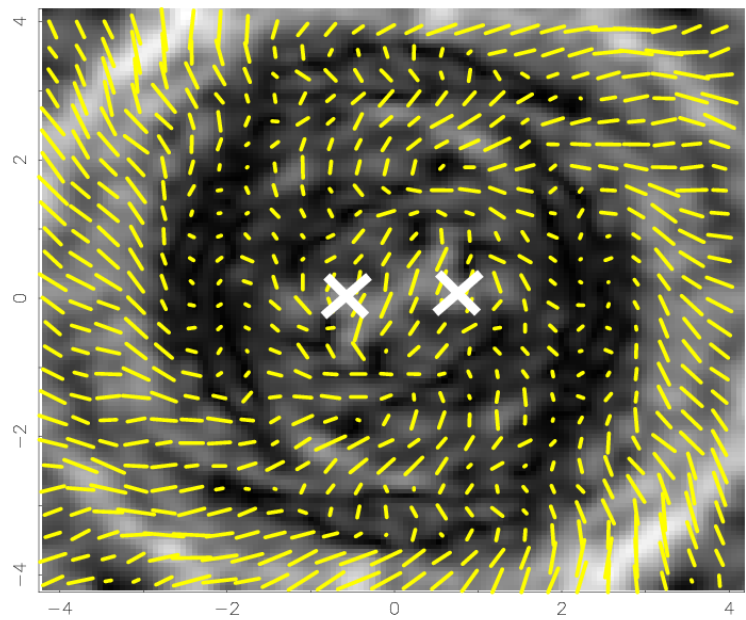
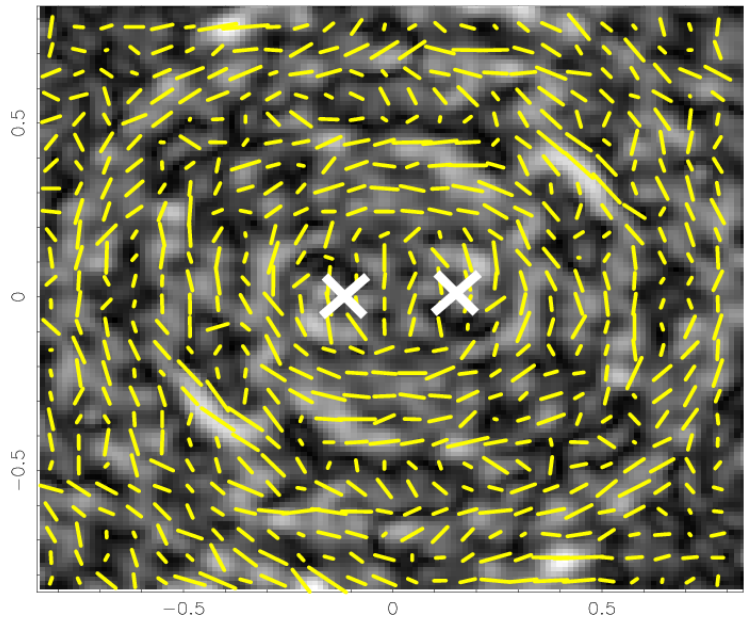
Probes higher-order biasing; constrains galaxy evolution models.

First detected on data by Simon et al. (2007) using the RCS survey.

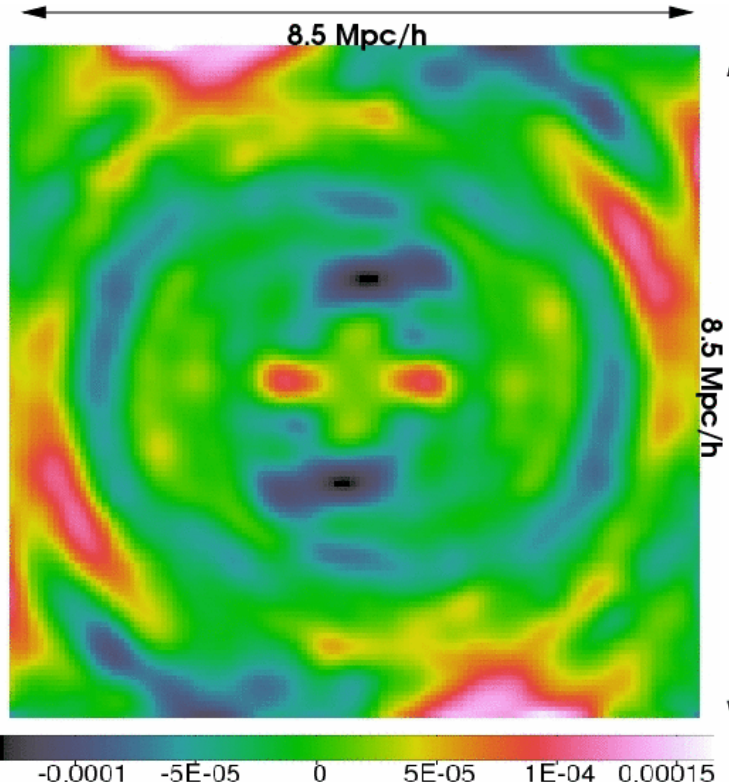
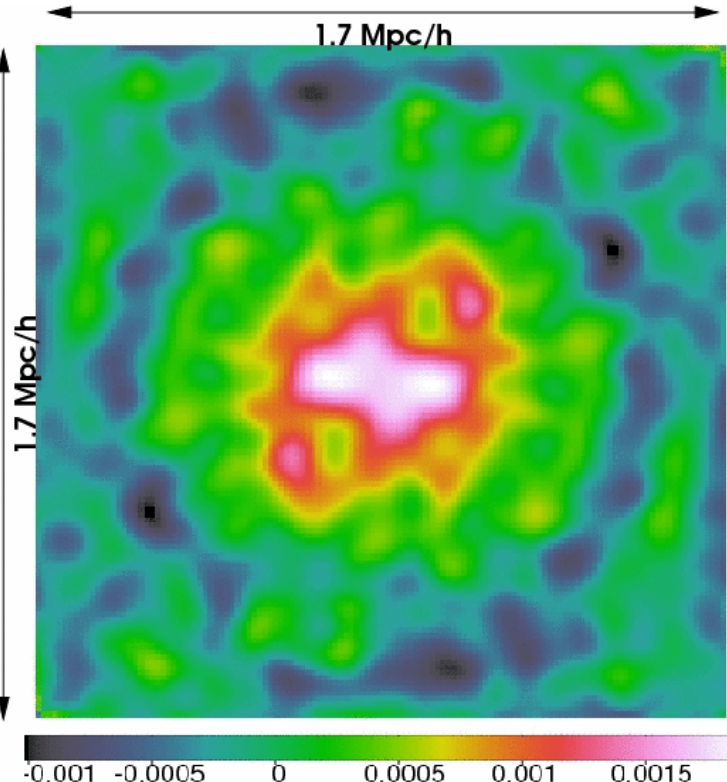




Shear around pairs of galaxies, by just taking the sum of shears associated with the two individual galaxies as determined by GGL (Simon et al. 2007)

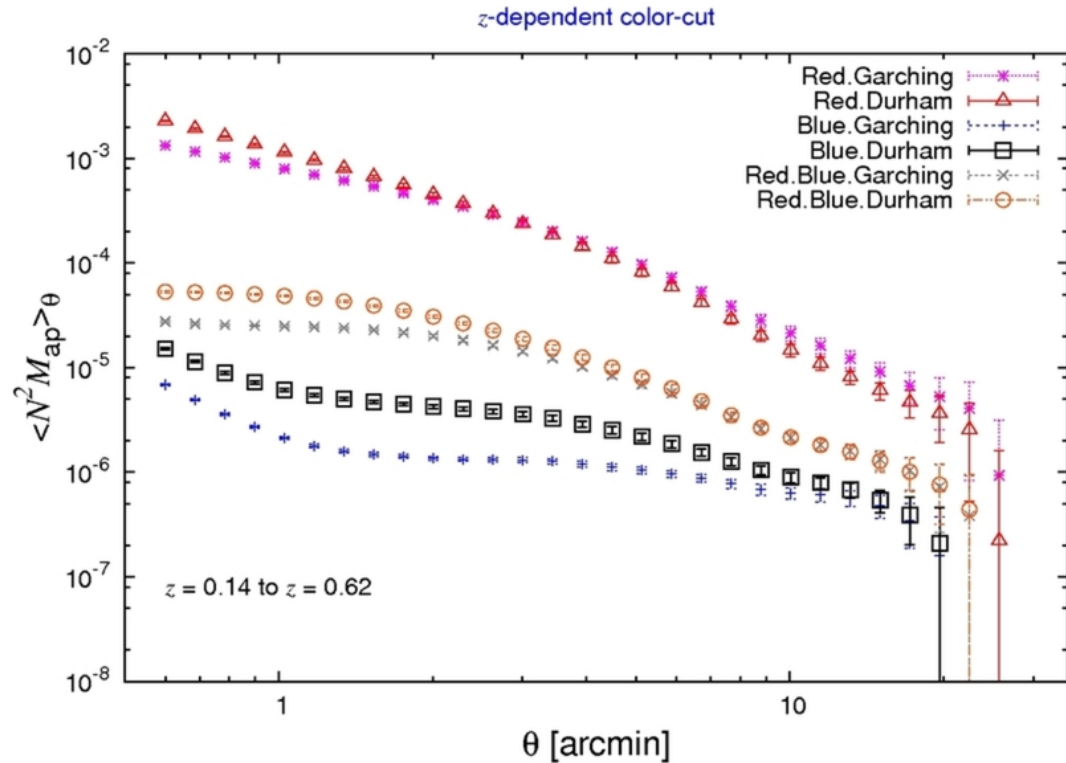


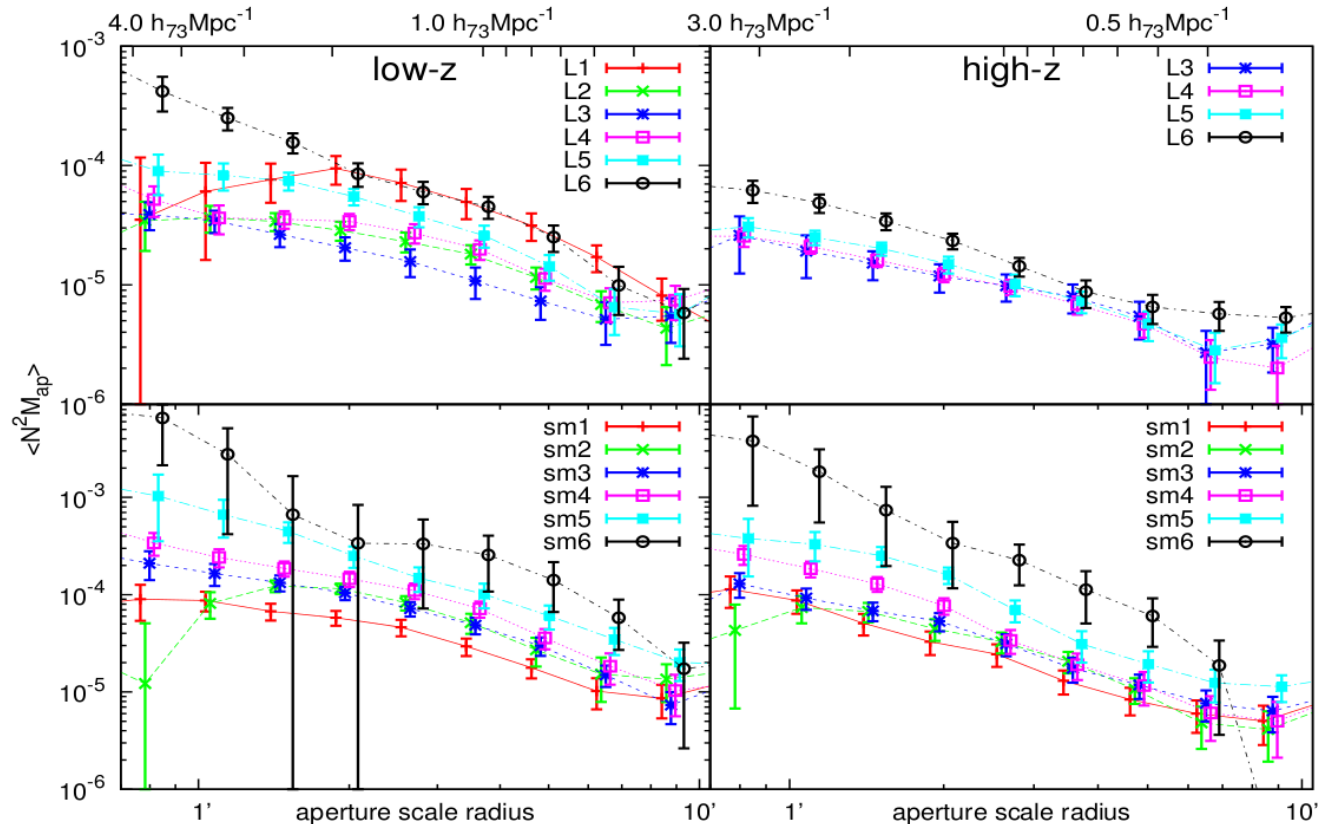
Shear around pairs of galaxies, with (shear from G1 + shear from G2 – as determined from the GGL signal) subtracted – i.e., excess shear over sum of the GGL signal (Simon et al. 2007)



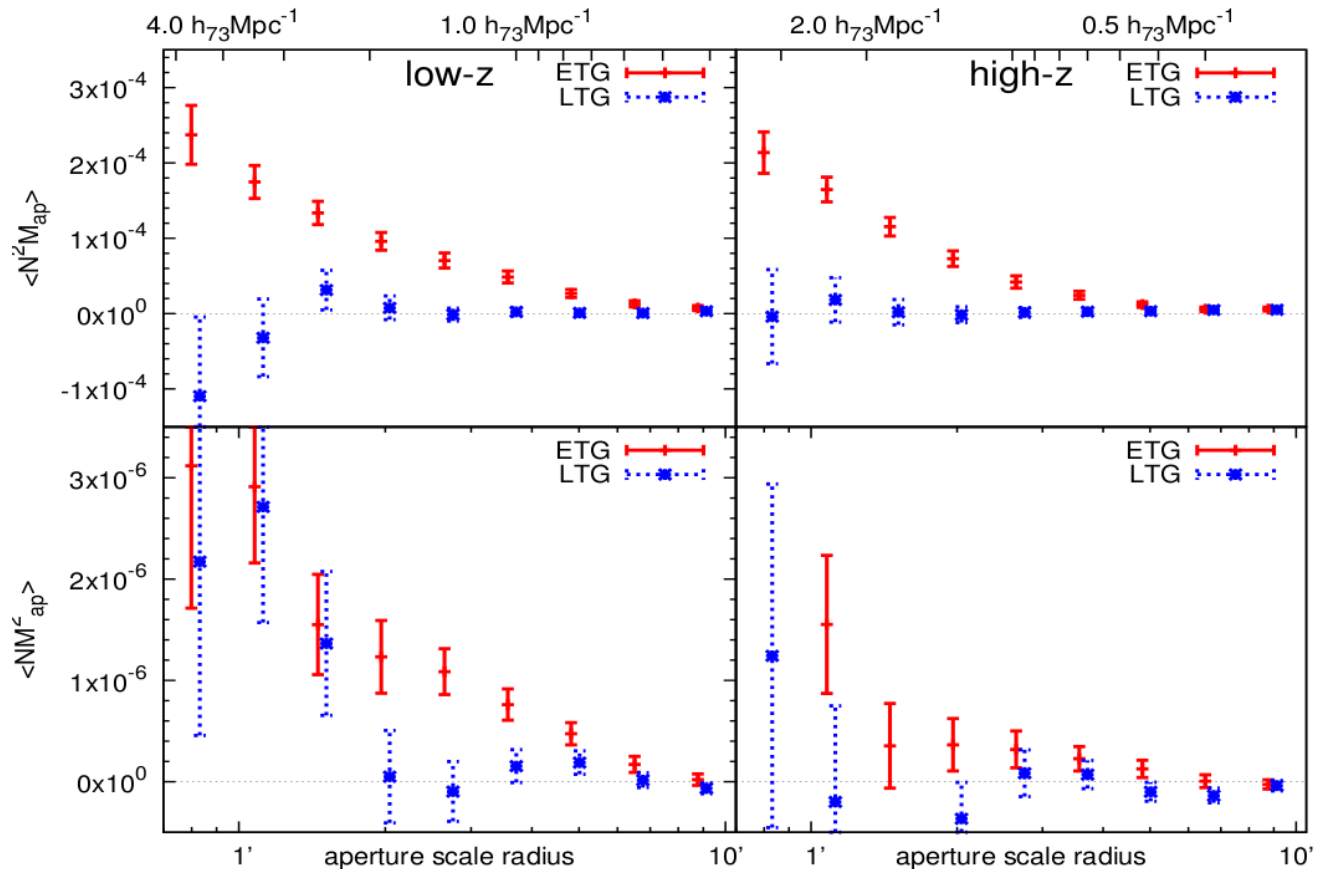
Mass reconstruction from the excess shear around galaxy pairs – i.e., excess mass around galaxy pairs over that of the sum of two galaxies (Simon et al. 2007)

Higher-order galaxy-shear correlations are highly sensitive probes of galaxy evolution models

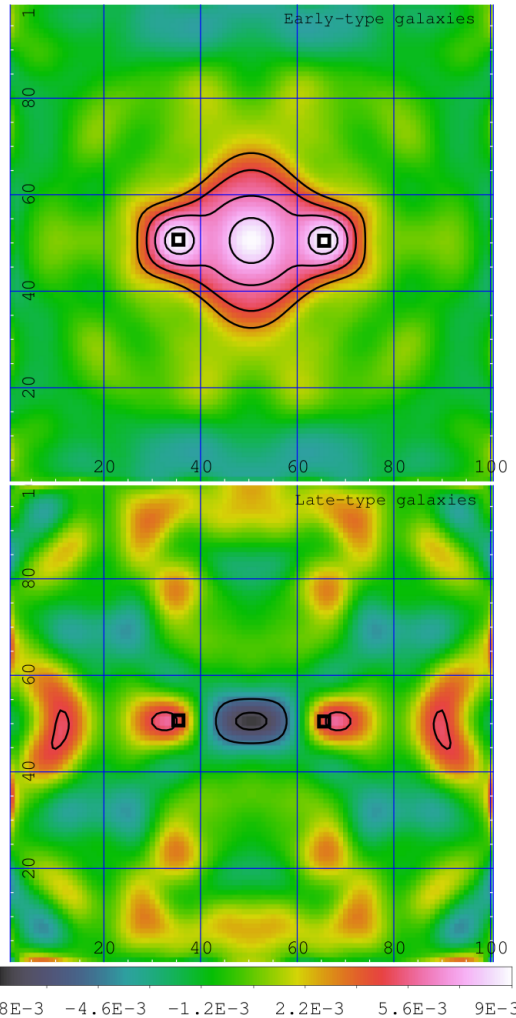




GGGL results from CFHTLenS collaboration (Simon et al. 2013)



Results from CFHTLenS collaboration (Simon et al. 2013)



Excess mass around pairs of galaxies –  
for early- (top) and late-type (bottom) galaxies,  
as measured from CFHTLenS (Simon et al. 2013);

(foreground) galaxy pairs have separation  
 $40'' \leq \Delta\theta \leq 60''$ ;

Excess mass profile around early-type galaxies  
clearly measured, whereas for late-type galaxies  
no significant excess is seen.

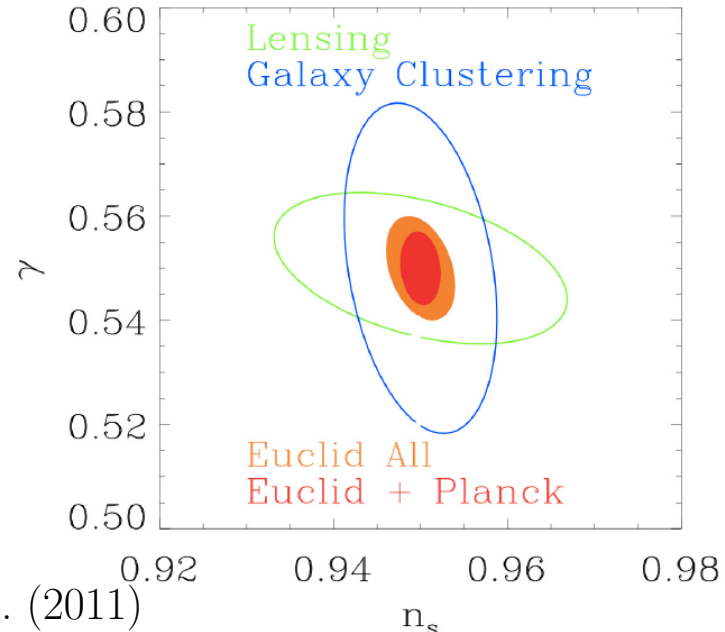
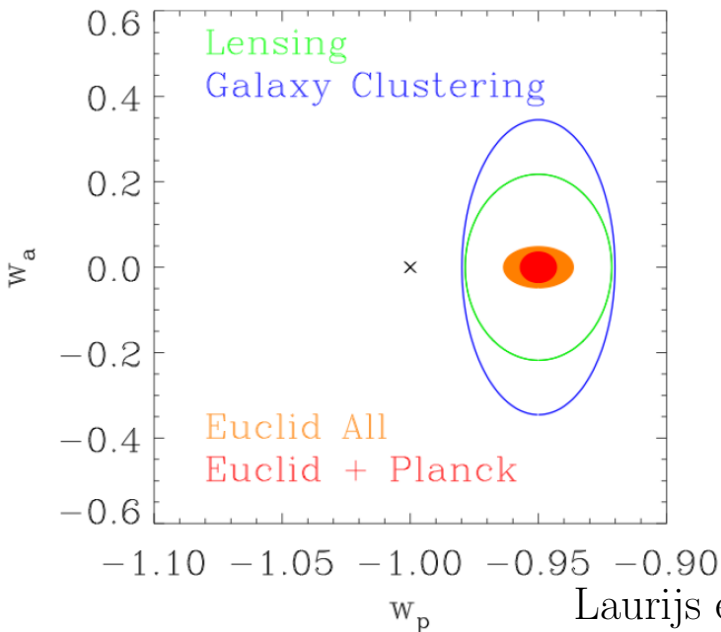
(Remember: Simulations indicate a very large difference in signal strength!)

# Conclusions

- Galaxy-galaxy lensing provides a unique tool for studying the relation between galaxies and mass.
- GGL signal easier to detect than cosmic shear, since it is linear in the shear (and less sensitive to certain systematics).
- GGL yields the (mean) halo mass of galaxies, as function of galaxy mass, luminosity and type.
- Galaxy bias and galaxy-mass correlation coefficient can be determined directly, by combining GGL with cosmic shear and galaxy correlation function.
- GGL and its generalizations offers a unique mean to determine mass properties of group and cluster halos.
- Higher-order galaxy-mass correlations detected with high significance; they are sensitive probe of galaxy evolution models.

# Future of cosmological weak lensing

- KiDS/VIKING, DES, HSC, EUCLID
- Lensing of the CMB (already detected)
- SKA – densely populating the radio sky; lensing of high-redshift 21 cm radiation



Laurijs et al. (2011)